Zweig rule violation in the scalar sector and values of low-energy constants

S. Descotes

JHEP HYPER VERSION

Received: *February 12, 2001,* Accepted: *March 1, 2001*

Zweig rule violation in the scalar sector and values of low-energy constants

Sébastien Descotes

IPN Groupe de Physique Théorique, Université Paris-Sud
91406 Orsay, France, and
Department of Physics and Astronomy, University of Southampton
Southampton SO17 1BJ, UK
E-mail: sdg@hep.phys.soton.ac.uk

Abstract: We discuss the role of the Zweig rule (ZR) violation in the scalar channel for the determination of low-energy constants and condensates arising in the effective chiral lagrangian of QCD. The analysis of the Goldstone boson masses and decay constants shows that the three-flavor condensate and some low-energy constants are very sensitive to the value of the ZR violating constant L_6. A similar study is performed in the case of the decay constants. A chiral sum rule based on experimental data in the 0^{++} channel is used to constrain L_6, indicating a significant decrease between the two- and the three-flavor condensates. The analysis of the scalar form factors of the pion at zero momentum suggests that the pseudoscalar decay constant could also be suppressed from $N_f = 2$ to 3.

Keywords: Spontaneous Symmetry Breaking, QCD, Chiral Lagrangians.

JHEP03(2001)002

Contents

1. Introduction

The low-energy constants (LEC's) of the effective chiral lagrangian of QCD [1] are quantities of great theoretical interest, since they reflect the way chiral symmetry is spontaneously broken. However, their determination remains a particularly awkward problem. In most cases [1]–[6], their values have been inferred from observables for the pseudoscalar mesons, with the help of two assumptions: (1) the quark condensate is the dominant order parameter to describe the Spontaneous Breakdown of Chiral Symmetry (SBχS) [1], and (2) the pattern of SBχS agrees correctly with a large-N_c description of QCD [7], in which quantum fluctuations are treated as small perturbations.

If we admit both assumptions, the SU(2) $\times$ SU(2) light quark condensate $\Sigma(2) = -\lim_{m_u,m_d\to 0}\langle\bar{u}u\rangle$ should not depend much on the mass of the strange quark. We could then set the latter to zero with no major effect on the condensate: $\Sigma(2) \sim \lim_{m_s\to 0}\Sigma(2) = \Sigma(3)$. We end up with only one large condensate in the SU(2)$\times$SU(2) and SU(3) $\times$ SU(3) chiral limits, which is not very sensitive to $\bar{q}q$ fluctuations. The LEC's suppressed by the Zweig rule, L_4 and L_6, are consistently supposed to be very small when considered at a typical hadronic scale.

However, several arguments may be raised against this "mean-field approximation" of SBχS, in which the Zweig rule applies and the chiral structure of QCD vacuum is more or less independent of the number of massless quarks. On the one hand, the scalar sector 0^{++} does not comply with large N_c-predictions [8], and some lattice simulations with dynamical fermions suggest a strong N_f-sensitivity of SBχS signals [9]. On the other hand, the behavior of the perturbative QCD β-function indicates that chiral symmetry should be restored for large enough values of N_f. In the vicinity ot the corresponding critical point, chiral order parameters should strongly vary with N_f. Various approaches, based on the investigation of the QCD conformal window [10], gap equations [11], or the instanton liquid model [12], have been proposed to investigate the variations of chiral order parameters with the number of massless flavors and to determine the critical value of N_f for the restoration of chiral symmetry.

In ref. [13], the N_f-sensitivity of chiral order parameters has been investigated without relying on perturbative methods, but rather by exploiting particular properties of vector-like gauge theories. The mechanism of SBχS is indeed related to

JHEP03(2001)002

the dynamics of the lowest eigenvalues of the Dirac operator: $\not{D} = \gamma_\mu(\partial_\mu + iG_\mu)$, considered on an euclidean torus [14, 15, 16]. Two main chiral order parameters can be expressed in this framework. The quark condensate Σ is related to the average density of eigenvalues around zero [14] and the pion decay constant in the chiral limit F can be interpreted as a conductivity [16]. The paramagnetic behavior of Dirac eigenvalues leads to a suppression of both order parameters when the number of flavors increases:

$$F^2(N_f+1) < F^2(N_f)\,, \qquad \Sigma(N_f+1) < \Sigma(N_f)\,. \tag{1.1}$$

This sensitivity of chiral order parameters to light-quark loops is suppressed in the large-N_c limit and is considered as weak for QCD according to the second hypothesis of the Standard framework. However, the N_f-dependence of chiral order parameters can be measured by correlators that violate the Zweig rule in the scalar (vacuum) channel. For instance, the difference $\Sigma(2) - \Sigma(3)$ (and the LEC L_6) is related to the correlator $\langle \bar{u}u\ \bar{s}s\rangle$ [17, 18] (this correlator can be interpreted as fluctuations of the density of Dirac eigenvalues [13]). The large ZR violation observed in the 0^{++} channel could therefore support a swift evolution in the chiral structure of the vacuum from $N_f = 2$ to $N_f = 3$. The quantum fluctuations of $\bar{q}q$ pairs would then play an essential role in the low-energy dynamics of QCD.

Hence, it is worth reconsidering the determination of LEC's without supposing (1) the dominance of the quark condensate and (2) the suppression of quantum fluctuations. This determination starts with the quark mass expansion of measured observables such as $F_\pi^2 M_\pi^2$ or $F_K^2 M_K^2$, using Chiral Perturbation Theory (χPT) [1]:

$$F_P^2 M_P^2 = m_q \Sigma_P + m_q^2[a_P + b_P \log(M_P)] + F_P^2 \delta_P\,, \tag{1.2}$$

where m_q denotes formally the masses of the light quarks u, d, s and the remainder $F_P^2\delta_P$ is of order m_q^3. The coefficients Σ_P, a_P, b_P are combinations of LEC's. The chiral logarithms $\log(M_P)$ stem from meson loops. The coefficient of each power of m_q does not depend on the renormalization scale of the effective theory ($F_P^2 M_P^2$ and m_q are independent of this scale).

Series like eq. (1.2) are assumed to converge on the basis of a genuine dimensional estimate [19]. The LEC's involved in the coefficients are related to Green functions of axial and vector currents, and scalar and pseudoscalar densities. The dimensional estimate consists in saturating the correlators by the exchange of resonances with masses of order $\Lambda_{\rm QCD}$ [4]. We obtain coefficients of order $\sim 1/\Lambda_{\rm QCD}^n$ for the power m_q^n. The quark mass expansion would therefore lead to (convergent) series in powers of $m_q/\Lambda_{\rm QCD} \ll 1$.

Notice that this genuine estimate cannot be applied to the linear term Σ_P corresponding to the quark condensate (there is no colored physical state to saturate $\langle\bar{q}q\rangle$). Moreover, the convergence of the whole series does not imply that the linear term Σ_P is dominant with respect to the quadratic term. In this article, we will

precisely address (1) the possibility of such a competition between the first two orders in the quark mass expansions, and (2) the implications of large values for the ZR-suppressed constants L_4 and L_6, in particular for the determination of LEC's.

Unfortunately, the masses and decay constants of the Goldstone bosons do not provide enough information to estimate the actual size of quantum fluctuations in QCD. To reach this goal, refs. [17, 18] have proposed a sum rule to estimate L_6 (or $\Sigma(2) - \Sigma(3)$) from experimental data in the scalar channel. Starting with Standard assumptions (two- and three-flavor condensates of large and similar sizes), ref. [17] ended up with a ratio $\Sigma(3)/\Sigma(2) \sim 1/2$ at the Standard $O(p^4)$ order, whereas ref. [18] confirmed a large decrease of the quark condensate when Standard $O(p^6)$ contributions were taken into account. Even though these results suggest a significant variation in the pattern of SBχS from $N_f = 2$ to $N_f = 3$, it seems necessary to reevaluate this sum rule without any supposition about the size of the condensates. This analysis will be performed in the second part of this article.

We will follow mainly the line of ref.[20], which can be considered as an orientation guide to this article. The first part is devoted to the determination of the LEC's from the pseudoscalar spectrum. Section 2 considers the role played by L_6 for the Goldstone boson masses and the quark condensates, whereas the decay constants and L_4 are treated in section 3. Section 4 deals mainly with the implication of ZR violation in the 0^{++} channel for the determination of LEC's. The second part of this article focuses on the estimate of L_6 from data in the scalar sector. Section 5 introduces the sum rule for L_6, sketches the Operator Product Expansion of the involved Green function and estimates the sum rule, with a special emphasis on the the scalar form factors of the pion and the kaon. In section 6, we present the results obtained for the quark condensates and LEC's from the sum rule, and we discuss two other quantities related to the pion scalar form factors: the slope of the strange form factor and the scalar radius of the pion. Section 7 sums up the main results of the article. Appendix A collects the expansions of pseudoscalar masses and decay constants in powers of quark masses. Appendix B deals with the Operator Product Expansion of the correlator $\langle \bar{u}u\ \bar{s}s \rangle$. Appendix C provides logarithmic derivatives of the pseudoscalar masses with respect to the quark masses.

2. Constraints from the pseudoscalar meson masses

2.1 Role of L_6

Let us first study the pseudoscalar masses M_π, M_K, M_η, starting from their expansion at the Standard $O(p^4)$ order, ref. [1, eqs. (10.7)]. We reexpress them as:

$$F_\pi^2 M_\pi^2 = 2m\Sigma(3) + 2m(m_s + 2m)Z^S + 4m^2 A + 4m^2 B_0^2 L + F_\pi^2 \delta_\pi \,, \tag{2.1}$$

$$F_K^2 M_K^2 = (m_s + m)\Sigma(3) + (m_s + m)(m_s + 2m)Z^S + \\ + (m_s + m)^2 A + m(m_s + m)B_0^2 L + F_K^2 \delta_K \,, \tag{2.2}$$

where $m = (m_u + m_d)/2$ and Z^S and A are scale-independent constants, containing respectively the LEC's $L_6(\mu)$ and $L_8(\mu)$,

$$Z^S = 32B_0^2 \left[L_6(\mu) - \frac{1}{512\pi^2} \left(\log \frac{M_K^2}{\mu^2} + \frac{2}{9} \log \frac{M_\eta^2}{\mu^2} \right) \right], \tag{2.3}$$

$$A = 16B_0^2 \left[L_8(\mu) - \frac{1}{512\pi^2} \left(\log \frac{M_K^2}{\mu^2} + \frac{2}{3} \log \frac{M_\eta^2}{\mu^2} \right) \right], \tag{2.4}$$

with $B_0 = \Sigma(3)/F_0^2$ and $F_0 \equiv F(3)$. The remaining $O(p^4)$ chiral logarithms are contained in L:[1]

$$L = \frac{1}{32\pi^2} \left[3 \log \frac{M_K^2}{M_\pi^2} + \log \frac{M_\eta^2}{M_K^2} \right] = 25.3 \cdot 10^{-3} \,. \tag{2.5}$$

There is a similar equation for $F_\eta^2 M_\eta^2$:

$$\begin{aligned} F_\eta^2 M_\eta^2 = {} & \frac{2}{3}(2m_s + m)\Sigma + \frac{2}{3}(2m_s + m)(m_s + 2m)Z^S + \\ & + \frac{4}{3}(2m_s^2 + m^2)A + \frac{8}{3}(m_s - m)^2 Z^P + \frac{1}{3}B_0^2 L + F_\eta^2 \delta_\eta \,, \end{aligned} \tag{2.6}$$

with the scale-independent constant $Z^P = 16B_0^2 L_7$. A factor B_0 is included in the expression of A, Z_S and Z_P in terms of $L_{i=6,7,8}$, so that they do not diverge in the limit $\Sigma(3) \to 0$. The corresponding equations for the pseudoscalar decay constants F_P^2 ($P = \pi$, K, η) will be treated in section 3.1.

We take $F_P^2 M_P^2$ and F_P^2 as independent observables, in order to separate in a straightforward way the "mass" constants L_6, L_7, L_8 from L_4, L_5 that appear only in the expansion of decay constants F_P^2. There is a second argument supporting the choice of F_P^2 and $F_P^2 M_P^2$ as independent observables of the pseudoscalar spectrum. We expand observables in powers of quark masses, supposing a good convergence of the series. We have sketched in the introduction how a naive dimensional estimate justifies this assumption: LEC's are related to QCD correlation functions, which can be saturated by massive resonances, leading to series in (m_q/Λ_{QCD}). We should therefore expect good convergence properties for "primary" observables obtained directly from the low-energy behavior of QCD correlation functions, like F_P^2 and $F_P^2 M_P^2$. For such quantities, the higher-order remainders should thus remain small. On the other hand, we have to be careful when we deal with "secondary" quantities combining "primary" observables. The higher-order remainders may then have a larger influence. In particular, ratios of "primary" observables (like $M_P^2 = F_P^2 M_P^2 / F_P^2$) might be dangerous if higher-order terms turned out to be sizable (leading to untrustworthy approximations like $1/(1+x) \simeq 1 - x$ with a large x).

[1] In this article, we use the following values of masses and decay constants: $M_\pi = 135\,\mathrm{MeV}$, $M_K = 495\,\mathrm{MeV}$, $M_\eta = 547\,\mathrm{MeV}$, $F_\pi = 92.4\,\mathrm{MeV}$, $F_K/F_\pi = 1.22$.

In eqs. (2.1), (2.2) and (2.6), all terms linear and quadratic in quark masses are shown. The remaining contributions, of order $O(m^3_{\rm quark})$ and higher, are collected in the remainders δ_P. We can consider that the latter are given to us, so that eqs. (2.1), (2.2) and (2.6) can be seen as algebraic identities relating the 3-flavor condensate $\Sigma(3)$ the quark mass ratio $r = m_s/m$, and the LEC's F_0, $L_6(\mu)$, L_7 and $L_8(\mu)$. The three-flavor quark condensate is measured in physical units, using the Gell-Mann–Oakes ratio: $X(3) = 2m\Sigma(3)/(F_\pi M_\pi)^2$ [21].

We are going to assume that the remainders δ_P are small ($\delta_P \ll M_P^2$), and investigate then the consequences of eqs. (2.1) and (2.2) for the values of LEC's. Before starting, we should comment the status of eqs. (2.1), (2.2) and (2.6) with respect to Chiral Perturbation Theory (χPT). Even if we imposed $\delta_P = 0$, we would not work in the frame of one-loop Standard χPT [1]: we do not suppose that the condensate $\Sigma(3)$ is dominant in these equations, we do not treat $1 - X(3)$ as a small expansion parameter, and accordingly, we do not replace (for instance) $2mB_0$ by M_π^2 in higher-order terms. However, we are not following Generalized χPT either [22], since B_0 is not treated as an expansion parameter: even with $\delta_P = 0$, eqs. (2.1), (2.2) and (2.6) exceed the Generalized tree level, since these equations include chiral logarithms.

It is useful to rewrite eqs. (2.1) and (2.2) as:

$$\frac{2m}{F_\pi^2 M_\pi^2}[\Sigma(3) + (2m + m_s)Z^S] = 1 - \tilde\epsilon(r) - \frac{4m^2B_0^2}{F_\pi^2 M_\pi^2}\frac{rL}{r-1} - \delta\,, \tag{2.7}$$

$$\frac{4m^2A}{F_\pi^2 M_\pi^2} = \tilde\epsilon(r) + \frac{4m^2B_0^2}{F_\pi^2 M_\pi^2}\frac{L}{r-1} + \delta'\,, \tag{2.8}$$

with

$$\tilde\epsilon(r) = 2\frac{\tilde r_2 - r}{r^2-1}, \qquad \tilde r_2 = 2\left(\frac{F_K M_K}{F_\pi M_\pi}\right)^2 - 1 \sim 39\,. \tag{2.9}$$

δ and δ' are linear combinations of the remainders δ_π and δ_K:

$$\begin{aligned}\delta &= \frac{r+1}{r-1}\frac{\delta_\pi}{M_\pi^2} - \left(\tilde\epsilon + \frac{2}{r-1}\right)\frac{\delta_K}{M_K^2}\,,\\ \delta' &= \frac{2}{r-1}\frac{\delta_\pi}{M_\pi^2} - \left(\tilde\epsilon + \frac{2}{r-1}\right)\frac{\delta_K}{M_K^2}\,.\end{aligned} \tag{2.10}$$

For large r, we expect $\delta' \ll \delta \sim \delta_\pi/M_\pi^2$. Similarly to ref. [6], we consider as parameters $F_0 = \lim_{m,m_s\to 0} F_\pi$ (i.e. $L_4(\mu)$), the ZR violating constant $L_6(\mu)$ and the quark mass ratio $r = m_s/m$. Eq. (2.7) ends up with a non-perturbative formula (no expansion) for the three-flavor Gell-Mann–Oakes–Renner ratio $X(3)$:

$$X(3) = \frac{2m\Sigma(3)}{F_\pi^2 M_\pi^2} = \frac{2}{1 + [1 + \kappa(1 - \tilde\epsilon - \delta)]^{1/2}}(1 - \tilde\epsilon - \delta), \tag{2.11}$$

where κ contains $L_6(\mu)$:

$$\kappa = 64(r+2)\left(\frac{F_\pi M_\pi}{F_0^2}\right)^2 \left\{ L_6(\mu) - \frac{1}{256\pi^2}\left(\log\frac{M_K}{\mu} + \frac{2}{9}\log\frac{M_\eta}{\mu}\right) + \right. \\ \left. + \frac{rL}{16(r-1)(r+2)} \right\}. \tag{2.12}$$

Eq. (2.11) is an exact identity, useful if the remainder δ in eq. (2.10) is small, i.e. if the expansion of QCD correlators in powers of the quark masses m_u, m_d, m_s is globally convergent. It means that $\delta_P \ll M_P^2$ in eqs. (2.1) and (2.2), but the linear term in these equations (related to the condensate) does not need to dominate.

κ describes quantum fluctuations of the condensate, and actually $\kappa = O(1/N_c)$. $L_6(\mu)$ has to be fixed carefully to keep κ small. κ is equal to zero for $10^3 \cdot L_6 = -0.26$ at the scale $\mu = M_\rho$, which is close to the value usually claimed in Standard χPT analysis [3]. In this case, eq. (2.11) yields $X(3)$ near 1, unless the quark mass ratio r decreases significantly, leading to $\tilde{\epsilon} \to 1$. This effect is well-known in GχPT [22]: the minimal value of r (corresponding to $\tilde{\epsilon} = 1$ and $X(3) = 0$) is $\tilde{r}_1 = 2(F_K M_K)/(F_\pi M_\pi) - 1 \sim 8$. Notice that for these very small values of r, the combination of higher-order remainders δ cannot be neglected any more in eq. (2.11).

But quantum fluctuations can modify this picture: the number before the curly brackets in eq. (2.12) is very large (~ 5340 for $r = 26$ and $F_0 = 85\,\mathrm{MeV}$). Hence, even a small positive value of $L_6(M_\rho)$ can lead to a strong suppression of $X(3)$, whatever the value of $r = m_s/m$. This effect can be seen on figure 1, where $X(3)$ is plotted as a function of $L_6(M_\rho)$ for $r = 20$, $r = 25$, $r = 30$ and $F_0 = 85$ and $75\,\mathrm{MeV}$. The decrease of $X(3)$ is slightly steeper for lower values of F_0.

Once $X(3)$ is known, eq. (2.8) leads to $L_8(\mu)$:

$$L_8(\mu) = \frac{L}{r-1} + \frac{F_0^4}{F_\pi^2 M_\pi^2}\frac{\tilde{\epsilon}+\delta'}{[X(3)]^2} + \frac{1}{512\pi^2}\left\{\log\frac{M_K^2}{\mu^2} + \frac{2}{3}\log\frac{M_\eta^2}{\mu^2}\right\}. \tag{2.13}$$

This constant depends on L_6 only through $X(3)$. Notice that this dependence is smaller when F_0 decreases (L_8 depends actually on L_6 through B_0).

The ZR violating constant L_7 can be obtained from $F_\eta^2 M_\eta^2$ eq. (2.6):

$$L_7 = \frac{1}{32}\frac{F_0^4}{F_\pi^2 M_\pi^2}\left\{\frac{1}{(r-1)^2}\left[3F_\eta^2 M_\eta^2 + F_\pi^2 M_\pi^2 - 4F_K^2 M_K^2\right] - F_\pi^2 M_\pi^2 \tilde{\epsilon}(r)\right\} - \\ - \frac{r^2}{32(r-1)^2}\frac{F_0^4}{F_\pi^2 M_\pi^2}\left[3F_\eta^2\delta_\eta + \frac{8r}{r+1}F_K^2\delta_K + (2r-1)F_\pi^2\delta_\pi\right], \tag{2.14}$$

where F_η will be discussed in section 3.1. The pseudoscalar spectrum satisfies with a good accuracy the relation $3F_\eta^2 M_\eta^2 + F_\pi^2 M_\pi^2 = 4F_K^2 M_K^2$, which reduces at the leading order to the Gell-Mann–Okubo formula [23]. This relation leads to a strong correlation between A and Z_P: $A + 2Z_P \simeq 0$. This correlation can also be seen in

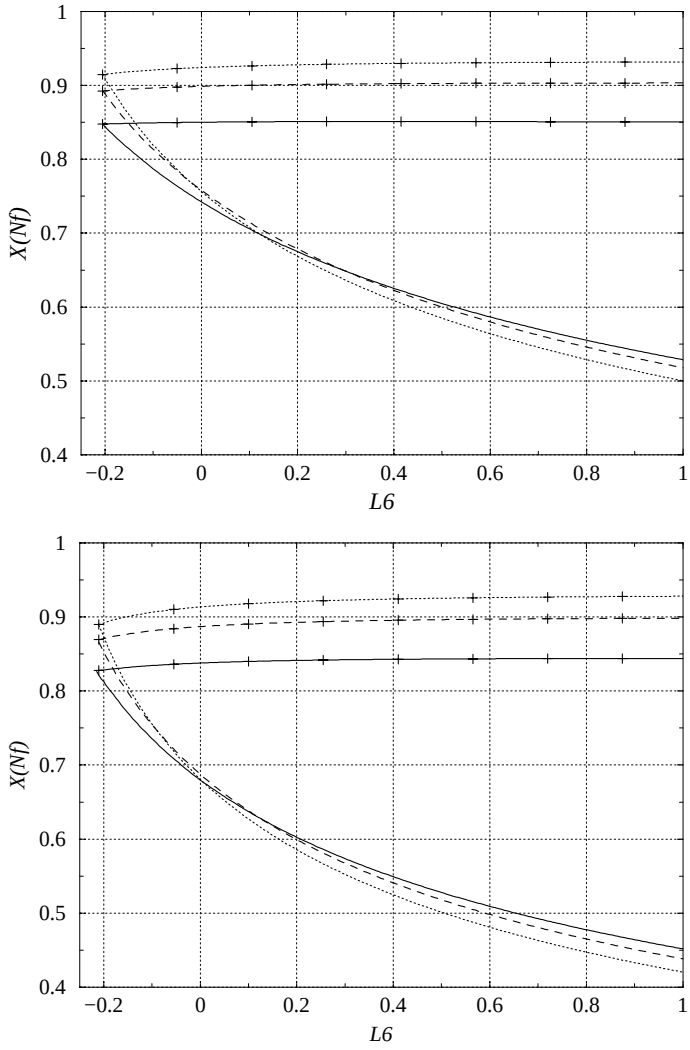

Figure 1: $X(2)$ (crosses) and $X(3)$ (no symbol) as functions of $L_6(M_\rho)\cdot 10^3$ and $r = m_s/m$ (solid line: $r = 20$, dashed line: $r = 25$, dotted line: $r = 30$) for $F_0 = 85\,\mathrm{MeV}$ (upper plot) and $75\,\mathrm{MeV}$ (lower plot).

Standard χPT between L_7 and L_8, and remains to be explained in both frameworks. No obvious reason forces this particular combination of two low-energy constants to be much smaller than the typical size of the effective constants.

2.2 Paramagnetic inequality for Σ

In ref. [13], $\bar{q}q$ fluctuations were shown to increase the two-flavor condensate $\Sigma(2) = -\lim_{m\to 0}\langle\bar{u}u\rangle|_{m_s \text{ physical}}$ with respect to $\Sigma(3)$, so that $X(2) > X(3)$. The two-flavor quark condensate can be obtained through the limit:

$$\Sigma(2) = \lim_{m\to 0}\frac{(F_\pi M_\pi)^2}{2m} = \Sigma(3) + m_s Z^S|_{m=0} + \delta_2\,, \tag{2.15}$$

keeping m_s fixed. We have the quantities: $\delta_2 = \lim_{m\to 0} F_\pi^2\delta_\pi/(2m)$ and $Z^S|_{m=0} =$

$Z^S + B_0^2 \Delta Z^S$, with:

$$\Delta Z^S = \frac{1}{16\pi^2}\left[\log\frac{M_K^2}{\bar{M}_K^2} + \frac{2}{9}\cdot\log\frac{M_\eta^2}{\bar{M}_\eta^2}\right], \tag{2.16}$$

and $\bar{M}_P^2 = \lim_{m\to 0} M_P^2$. The effect of ΔZ^S is very small.[2] ΔZ^S should be compared to the logarithmic terms included in Z^S, eq. (2.3), at a typical scale $\mu \sim M_\rho$. ΔZ^S reaches hardly 10% of this logarithmic piece.

Once Z^S is eliminated from eqs. (2.7) and (2.15), we obtain the two-flavor Gell-Mann–Oakes–Renner ratio $X(2) = 2m\Sigma(2)/(F_\pi M_\pi)^2$:

$$\begin{aligned} X(2) = {} & [1-\tilde{\epsilon}]\frac{r}{r+2} + \frac{2}{r+2}X(3) - \\ & - \frac{(F_\pi M_\pi)^2}{2F_0^4}X(3)^2\left[\frac{2r^2}{(r-1)(r+2)}L - r\Delta Z^S\right] + \delta_X\,, \end{aligned} \tag{2.17}$$

with:

$$\begin{aligned} \delta_X &= \delta_2 - \frac{r}{r+2}\delta \\ &= \frac{1}{F_\pi^2 M_\pi^2}\left[m\lim_{m\to 0}\frac{F_\pi^2\delta_\pi}{m} - \frac{r(r+1)}{(r+2)(r-1)}F_\pi^2\delta_\pi\right] + \frac{r}{r+1}\left(\tilde{\epsilon} + \frac{2}{r-1}\right)\frac{\delta_K}{M_K^2}\,. \end{aligned} \tag{2.18}$$

In the expression of δ_X, the remainders δ_P/M_P^2 are suppressed by a factor m/m_s: this suppression is obvious for δ_K ($\tilde{\epsilon} = O(1/r)$), whereas the operator applied to δ_π cancels the terms of order $O(mm_s^2)$. For $r > 20$, we expect thus $|\delta_X| \sim |\delta'|$. The dependence of $X(2)$ on L_6 is completely hidden in $X(3)$, and therefore marginal, as shown in figure 1.

The paramagnetic inequality $X(2) \geq X(3)$ constrains the maximal value reached by $X(3) = X(3)|_{\max}$. If we neglect $\delta\Sigma(2)$ in eq. (2.15), the inequality can be translated into a lower bound for L_6:

$$L_6(\mu) \geq \frac{1}{512\pi^2}\left(\log\frac{\bar{M}_K^2}{\mu^2} + \frac{2}{9}\log\frac{\bar{M}_\eta^2}{\mu^2}\right). \tag{2.19}$$

Figure 1 shows clearly the lower bound: $L_6(M_\rho) \geq -0.21\cdot 10^{-3}$.

$X(2)$ is loosely related to $X(3)$, but it is very strongly correlated with r, specially for small values of r. Eq. (2.17) yields the estimate $X(2) \sim [1-\tilde{\epsilon}]\cdot r/(r+2)$, up to small correcting terms due to $X(3)$. We are going to study the effect of these correcting terms.

If we neglect ΔZ^S, $X(2)$ is a quadratic function of $X(3)$, which is not monotonous when $X(3)$ varies from 0 to $X(3)|_{\max}$: it first increases, and then decreases (see figure 1). The decrease of $X(2)$ for $X(3)$ close to its upper bound is caused by the negative term, quadratic in $X(3)$, in eq. (2.17). This decrease of $X(2)$ is more significant for small F_0, because the factor in front of $[X(3)]^2$ in eq. (2.17) becomes larger.

[2] It can be evaluated following the procedure of section A.3.

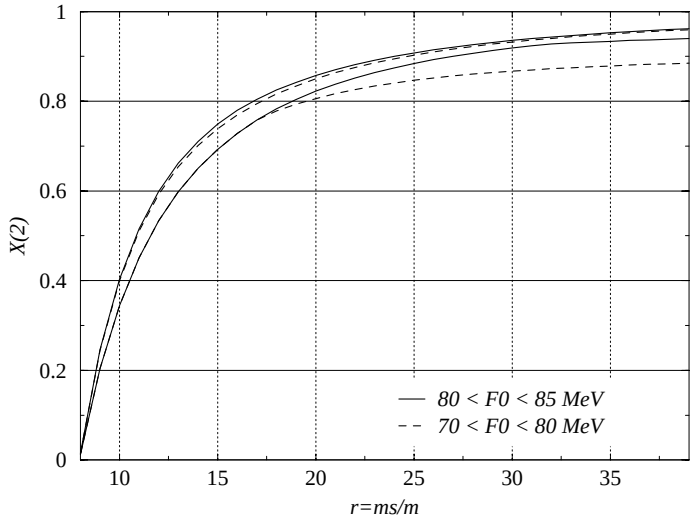

Figure 2: $X(2)$ as a function of r for two ranges of F_0

Therefore, $X(2)$ does not reach its maximum for the paramagnetic bound $X(2) = X(3)|_{\max}$, whereas its minimum is the smallest of the two values obtained for $X(3) = 0$ and $X(3) = X(3)|_{\max}$.[3] The dependence on r of the minimal value of $X(2)$ can be guessed rather easily. For large r, the term linear in $X(3)$ in eq. (2.17) can be neglected: the minimum of $X(2)$ occurs for $X(3) = X(3)|_{\max}$. For small r, $X(2)$ and $X(3)$ tend to 0, and the term quadratic in $X(3)$ should be small with respect to the linear term. Therefore, $X(2)$ reaches its minimum for $X(3) = 0$ when r is small.

The numerical analysis of eq. (2.17), including ΔZ^S, supports this intuitive description. In figure 2, the variation ranges of $X(2)$ are plotted for several values of F_0. The curve for the minimum of $X(2)$ exhibits a cusp when the minimum of $X(2)$ corresponds no more to $X(3) = 0$, but to $X(3)|_{\max}$. $X(2)$ appears to be strongly correlated to r, even though a large value of $X(2) \sim 0.9$ can be associated to a broad range of r.

3. Constraints from the pseudoscalar decay constants

3.1 Role of L_4

The decomposition used for the Goldstone boson masses can be adapted to the decay constants:

$$F_\pi^2 = F_0^2 + 2m\xi + 2(2m + m_s)\tilde{\xi} + \qquad (3.1)$$
$$+\frac{1}{16\pi^2}\frac{F_\pi^2 M_\pi^2}{F_0^2}X(3)\left[2\log\frac{M_K^2}{M_\pi^2} + \log\frac{M_\eta^2}{M_K^2}\right] + \varepsilon_\pi,$$
$$F_K^2 = F_0^2 + (m + m_s)\xi + 2(2m + m_s)\tilde{\xi} + \frac{1}{2}\frac{F_\pi^2 M_\pi^2}{F_0^2}X(3)L + \varepsilon_K\,, \qquad (3.2)$$

[3] This updates ref. [13], where the minimum and maximum of $X(2)$ were claimed to be obtained for $X(3) = 0$ and $X(3) = X(3)|_{\max}$.

with the scale-independent constants related to L_4 and L_5:

$$\xi = 8B_0 \left[L_5(\mu) - \frac{1}{256\pi^2} \left(\log \frac{M_K^2}{\mu^2} + 2 \log \frac{M_\eta^2}{\mu^2} \right) \right], \tag{3.3}$$

$$\tilde{\xi} = 8B_0 \left[L_4(\mu) - \frac{1}{256\pi^2} \log \frac{M_K^2}{\mu^2} \right], \tag{3.4}$$

eqs. (3.1) and (3.2) contain all the terms constant or linear in quark masses in the expansion of F_π^2 and F_K^2, whereas ε_P denote remainders of order $O(m^2_{\rm quark})$. There is also a formula for F_η, which can be written as:

$$\begin{aligned} F_\eta^2 = {} & \frac{4}{3} F_K^2 - \frac{1}{3} F_\pi^2 + \frac{1}{24\pi^2} \frac{M_\pi^2 F_\pi^2}{F_0^2} r X(3) \log \frac{M_\eta^2}{M_K^2} + \\ & + \frac{1}{48\pi^2} \frac{M_\pi^2 F_\pi^2}{F_0^2} X(3) \left(\log \frac{M_\eta^2}{M_K^2} - \log \frac{M_K^2}{M_\pi^2} \right) + \varepsilon_\eta - \frac{4}{3} \varepsilon_K + \frac{1}{3} \varepsilon_\pi \,. \end{aligned} \tag{3.5}$$

The two scale-independent constants can be extracted from eqs. (3.1) and (3.2):

$$\begin{aligned} \frac{2m\xi}{F_\pi^2} = {} & \tilde{\eta}(r) + \frac{1}{32\pi^2} \frac{F_\pi^2}{F_0^2} \frac{M_\pi^2}{F_\pi^2} \frac{X(3)}{r-1} \left[5 \log \frac{M_K^2}{M_\pi^2} + 3 \log \frac{M_\eta^2}{M_K^2} \right] + \\ & + \frac{2}{r-1} \left[\frac{\varepsilon_\pi}{F_\pi^2} - \frac{\varepsilon_K}{F_\pi^2} \right] \end{aligned} \tag{3.6}$$

$$\begin{aligned} \frac{2m\tilde{\xi}}{F_\pi^2} = {} & \frac{1}{r+2} \left\{ 1 - \tilde{\eta}(r) - \frac{F_0^2}{F_\pi^2} - \right. \\ & \left. - \frac{1}{32\pi^2} \frac{F_\pi^2}{F_0^2} \frac{M_\pi^2}{F_\pi^2} X(3) \left[\frac{4r+1}{r-1} \log \frac{M_K^2}{M_\pi^2} + \frac{2r+1}{r-1} \log \frac{M_\eta^2}{M_K^2} \right] \right\} + \\ & + \frac{1}{r+2} \left[\frac{2}{r-1} \frac{\varepsilon_K}{F_\pi^2} - \frac{r+1}{r-1} \frac{\varepsilon_\pi}{F_\pi^2} \right], \end{aligned} \tag{3.7}$$

with:

$$\tilde{\eta}(r) = \frac{2}{r-1} \left(\frac{F_K^2}{F_\pi^2} - 1 \right) \sim \frac{0.977}{r-1} \,, \tag{3.8}$$

where the latter estimate is obtained for $F_K/F_\pi = 1.22$.

ξ (i.e. L_5) turns out to depend essentially on $X(3)$ and r, whereas $\tilde{\xi}$ (i.e. L_4) is related to the difference between $F(3)$ and F_π. Eq. (3.7) leads to a quadratic equation for $[F(3)/F_\pi]^2$, involving L_4:

$$\left(\frac{F(3)}{F_\pi} \right)^4 - (1 - \tilde{\eta} - \varepsilon) \left(\frac{F(3)}{F_\pi} \right)^2 + \lambda X(3) = 0 \,, \tag{3.9}$$

with:

$$\lambda = 8(r+2)\frac{M_\pi^2}{F_\pi^2}\left\{L_4(\mu) - \frac{1}{256\pi^2}\log\frac{M_K^2}{\mu^2} + \right.$$
$$\left. + \frac{1}{256\pi^2}\frac{1}{(r+2)(r-1)}\left[(4r+1)\log\frac{M_K^2}{M_\pi^2} + (2r+1)\log\frac{M_\eta^2}{M_K^2}\right]\right\},$$
$$\varepsilon = \frac{r+1}{r-1}\frac{\varepsilon_\pi}{F_\pi^2} - \left(\tilde{\eta} + \frac{2}{r-1}\right)\frac{\varepsilon_K}{F_K^2}\,. \tag{3.10}$$

Eq. (3.9) has the solution:

$$\left(\frac{F(3)}{F_\pi}\right)^2 = \frac{1-\tilde{\eta}-\varepsilon+\sqrt{(1-\tilde{\eta}-\varepsilon)^2 - 4\lambda X(3)}}{2}\,. \tag{3.11}$$

Notice that this formula is very close to eq. (2.11), that relates $X(3)$ to $L_6(\mu)$ through the parameter κ. For $r = 25$, the factor in front of the curly brackets in the definition of λ is of order 460, and λ vanishes for $L_4(M_\rho) = -0.51 \cdot 10^{-3}$.

Eq. (3.9) admits a solution only if $\lambda X(3) \leq (1-\tilde{\eta}-\varepsilon)^2/4$. From eq. (3.11), we get then a range for $F(3)$:

$$\frac{1-\tilde{\eta}-\varepsilon}{2} \leq \left(\frac{F(3)}{F_\pi}\right)^2 \leq 1-\tilde{\eta}-\varepsilon\,. \tag{3.12}$$

The variations of $F(3)$ with $L_4(M_\rho)$ are plotted for three values of r and $X(3) = 0.9$ and 0.5 in figure 3. When $X(3)$ decreases, the allowed range for L_4 broadens. This is due to the definition of L_4, which relates $B_0 L_4 = \Sigma(3)L_4/F^2(3)$ to the low-energy behavior of a QCD Green function. $[F(3)/F_\pi]^2$ starts at 0.9 (for the lowest possible value of $L_4(M_\rho)$) and decreases until 0.5. $F(3)$ can thus vary from 87 to 65 MeV, depending on the value of $L_4(M_\rho)$.

3.2 Paramagnetic inequality for F^2

We obtain $F(2)$ by taking the limit:

$$F^2(2) = \lim_{m\to 0} F_\pi^2 = F(3)^2 + 2m_s\tilde{\xi}|_{m=0} + \varepsilon_2\,, \tag{3.13}$$

keeping m_s fixed. We have $\varepsilon_2 = \lim_{m\to 0}\varepsilon_\pi$ and $\tilde{\xi}|_{m=0} = \tilde{\xi} + B_0\Delta\tilde{\xi}$, with

$$\Delta\tilde{\xi} = \frac{1}{32\pi^2}\log\frac{M_K^2}{\bar{M}_K^2}\,. \tag{3.14}$$

$\Delta\tilde{\xi}$ has a tiny effect on the results, similarly to ΔZ^S for $X(3)$. We get the equation:

$$\left[\frac{F(2)}{F_\pi}\right]^2 = \frac{r}{r+2}\left\{[1-\tilde{\eta}] + \frac{2}{r}\left[\frac{F(3)}{F_\pi}\right]^2 - X(3)\phi\left[\frac{F_\pi}{F(3)}\right]^2 - \varepsilon_F\right\}, \tag{3.15}$$

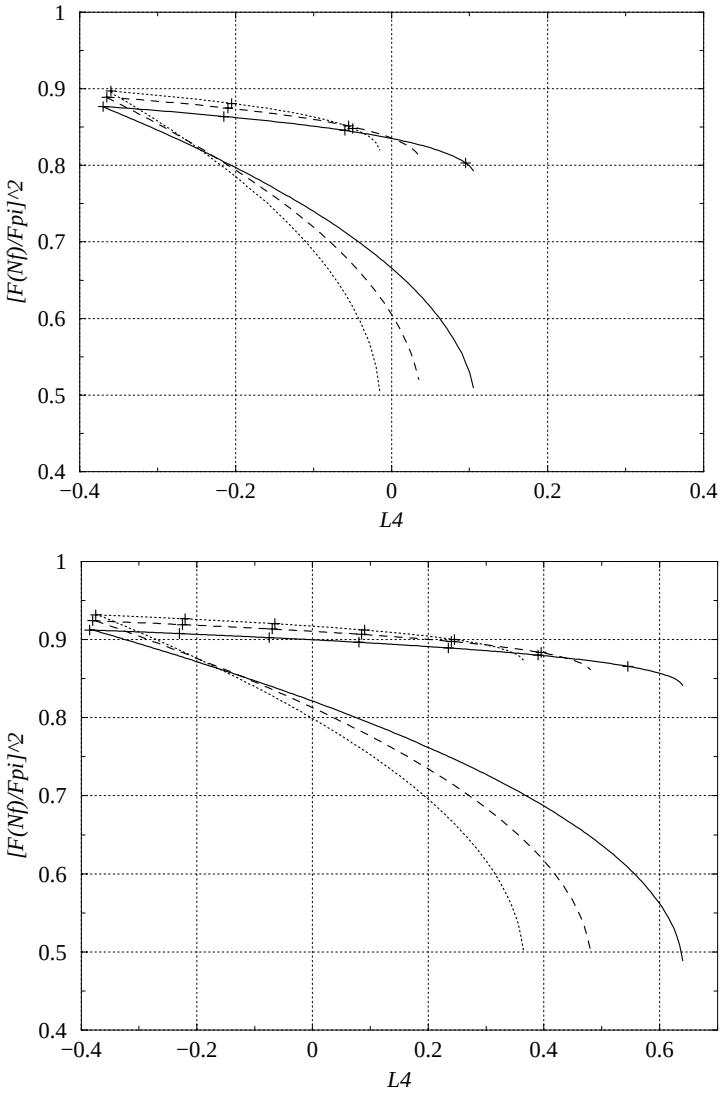

Figure 3: $F(2)$ (crosses) and $F(3)$ (no symbol) as functions of $L_4(M_\rho)\cdot 10^3$ and $r = m_s/m$ (solid lines: $r = 20$, dashed lines: $r = 25$, dotted lines: $r = 30$) for $X(3)$=0.9 (upper plot) and 0.5 (lower plot).

with:

$$\begin{aligned}
\varepsilon_F &= \frac{r+1}{r-1}\frac{\varepsilon_\pi}{F_\pi^2} - \frac{r+2}{r}\frac{\varepsilon_2}{F_\pi^2} - \left(\tilde{\eta} + \frac{2}{r-1}\right)\frac{\varepsilon_K}{F_K^2} \\
&= \frac{1}{F_\pi^2}\left[\frac{r+1}{r-1}\varepsilon_\pi - \frac{r+2}{r}\lim_{m\to 0}\varepsilon_\pi\right] - \left(\tilde{\eta} + \frac{2}{r-1}\right)\frac{\varepsilon_K}{F_K^2}, \\
\phi &= \frac{1}{32\pi^2}\frac{M_\pi^2}{F_\pi^2}\left[\frac{4r+1}{r-1}\log\frac{M_K^2}{M_\pi^2} + \frac{2r+1}{r-1}\log\frac{M_\eta^2}{M_K^2} + (r+2)\log\frac{\bar{M}_K^2}{M_K^2}\right]. \quad (3.16)
\end{aligned}$$

It is interesting to compare the expression of $F(2)$ as a function of $F(3)$ with eq. (2.17) that relates $X(2)$ to $X(3)$. Even though the equations look rather similar, we can

	$F(3)$ [MeV]		$F(2)$ [MeV]		No ZR violation	
r	min	max	min	max	F [MeV]	X
10	61.69	87.24	81.31	87.24	85.57	0.403
15	63.02	89.12	82.34	89.12	86.17	0.751
20	63.63	89.99	83.02	89.99	86.71	0.860
25	63.99	90.50	83.38	90.50	87.08	0.905
30	64.23	90.83	83.43	90.83	87.35	0.928
35	64.39	91.06	83.14	91.06	87.55	0.940

Table 1: On the left hand-side, bounds for $F(3)$. In the middle, corresponding bounds for $F(2)$. On the right hand-side, values of $F(3)$ and $X(3)$ saturating both paramagnetic inequalities: $F(2) = F(3)$ and $X(2) = X(3)$.

notice that eq. (2.17) is a quadratic function of $X(3)$ whereas eq. (3.15) involves $[F(3)/F_\pi]^2$ and its inverse $[F_\pi/F(3)]^2$. Moreover, eq. (3.15) is an increasing function of $F(3)$, whereas $X(2)$ is not monotonous with $X(3)$. On the other hand, ε_F suppresses the remainders ε_P/F_P^2 by a factor m/m_s, in a comparable way to δ_X.

The paramagnetic inequality $F(2) \geq F(3)$ is translated into an upper bound for $F(3)$:

$$\left(\frac{F(3)}{F_\pi}\right)^2 \leq \frac{1-\tilde{\eta}-\varepsilon_F+\sqrt{(1-\tilde{\eta}-\varepsilon_F)^2-4\phi X(3)}}{2}\,. \tag{3.17}$$

A quick estimate shows that the condition $X(3) \leq (1-\tilde{\eta}-\varepsilon_F)^2/(4\phi)$ is satisfied for any r between $\tilde{r}_1 \sim 8$ and $\tilde{r}_2$. This paramagnetic bound corresponds to a lower bound for $L_4(\mu)$:

$$L_4(\mu) > \frac{1}{256\pi^2}\log\frac{\bar{M}_K^2}{\mu^2}\,. \tag{3.18}$$

The term $\log(\bar{M}_K^2)$ is very weakly dependent on r, $X(3)$ and $F(3)$. If we scan the acceptable range of variation for these three parameters, we obtain the lower bound $L_4(M_\rho) > -0.37\cdot 10^{-3}$. We notice that the curves for $F(2)$ and $F(3)$ cross each other at this value in figure 3.

Since $\phi > 0$, eqs. (3.12) and (3.17) lead to the range:

$$\frac{1-\tilde{\eta}-\varepsilon}{2} \leq \frac{F(3)^2}{F_\pi^2} \leq 1-\tilde{\eta}-\max(\varepsilon_F,\varepsilon). \tag{3.19}$$

The bounds on $F(3)$ are indicated in table 1 (neglecting the remainders ε and ε_F). Table 1 collects for several values of r the corresponding bounds for $F(2)$, obtained using eq. (3.15). It gives also the values of $X(3)$ and $F(3)$ that saturate both paramagnetic bounds: $F(2) = F(3)$ and $X(2) = X(3)$. In this case, the Zweig rule would be violated neither for the masses nor for the decay constants.

4. Sensitivity of low-energy constants to ZR violation

The equations (2.13), (2.14), (3.6) and (3.7) can be used to extract the LEC's $L_{i=4,5,7,8}$ as functions of r, F_0 et $X(3)$, or equivalently, of L_6, $F_0 \equiv F(3)$ and r using eq. (2.11). Results are shown in table 2 as a function of L_6, for 2 values of F_0 and 3 values of r.

This table has been obtained by neglecting the higher-order terms δ_P and ϵ_P, which start at the next-to-next-to-leading order (NNLO). If the size of these remainders is large, the values collected in these tables should be clearly modified. If we keep considering the low-energy constants as functions of $L_6(M_\rho)$ and we change the relative size of the NNLO remainders within a range of 5%, the corresponding variations of $X(3)$ are of order ± 0.02. The impact on the other LEC's is larger for smaller $X(3)$ (of order $\pm 0.3 \cdot 10^{-3}$ for $X(3) \sim 0.8$, $r \sim 25$).

The authors of ref. [6] have estimated the NNLO remainders in the Standard Framework. The authors assume first $L_4(M_\rho) = L_6(M_\rho) = 0$ and $r = 24$, estimate $O(p^6)$ counterterms (Standard counting) through a saturation of the associated correlators by resonances, and fit globally on the available data (masses, decay constants, form factors). For the decay constants, the obtained NNLO remainders ϵ_P are less than 5%. The situation is less clear for the masses, due to a bad convergence of the series. For instance, ref. [6] has obtained the decomposition: $M_\pi^2/(M_\pi^2)_{\rm phys} = 0.746 + 0.007 + 0.247$, where the three terms correspond respectively to the leading $O(m)$, next-to-leading $O(m^2)$ and next-to-next-to-leading $O(m^3)$ orders. Ref. [6] suggested that a variation of $L_4(M_\rho)$ and $L_6(M_\rho)$ could make the NNLO contribution decrease, but a competition occurs then between the $O(m^2)$ term and the leading-order term.

Such a competition could be understood from our analysis as a consequence of the suppression of the three-flavor condensate $X(3)$. It would be of great interest to

	$r = 20$				$r = 25$				$r = 30$			
L_6	4	5	7	8	4	5	7	8	4	5	7	8
−0.2	−0.284	2.410	−1.259	2.624	−0.282	1.603	−0.503	0.994	−0.284	1.130	−0.185	0.298
−0.1	−0.264	2.628	−1.452	3.044	−0.261	1.812	−0.604	1.224	−0.262	1.332	−0.233	0.416
0.	−0.246	2.824	−1.636	3.445	−0.242	1.993	−0.699	1.440	−0.243	1.501	−0.276	0.525
0.2	−0.215	3.167	−1.986	4.207	−0.210	2.306	−0.880	1.848	−0.211	1.790	−0.360	0.730
0.4	−0.188	3.466	−2.318	4.930	−0.184	2.572	−1.050	2.232	−0.184	2.036	−0.439	0.925
1.	−0.121	4.209	−3.256	6.966	−0.116	3.228	−1.532	3.314	−0.117	2.631	−0.664	1.471
−0.2	0.068	1.833	−0.816	1.653	−0.013	1.174	−0.325	0.586	−0.065	0.782	−0.117	0.124
−0.1	0.133	2.088	−0.999	2.056	0.053	1.414	−0.420	0.804	0.002	1.014	−0.161	0.236
0.	0.190	2.310	−1.176	2.442	0.108	1.616	−0.509	1.008	0.055	1.203	−0.202	0.340
0.2	0.287	2.684	−1.503	3.156	0.200	1.953	−0.678	1.391	0.144	1.513	−0.290	0.533
0.4	0.368	3.002	−1.814	3.833	0.277	2.234	−0.837	1.751	0.217	1.770	−0.354	0.715
1.	0.567	3.781	−2.696	5.751	0.463	2.915	−1.291	2.774	0.392	2.384	−0.565	1.232

Table 2: Low-energy constants $L_i(M_\rho) \cdot 10^3$ as functions of $L_6(M_\rho) \cdot 10^3$ and $r = m_s/m$, for $F_0 = 85\,\text{MeV}$ (upper part) and $75\,\text{MeV}$ (lower part).

proceed to the same analysis as in ref. [6], and to allow a competition between the terms linear and quadratic in quark masses. This might improve the convergence of the expansion of Goldstone boson observables in powers of quark masses. Even if the three-flavor condensate $X(3)$ is suppressed (first term of the series for pseudoscalar masses), we expect a global convergence of the series, i.e. small higher-order remainders δ_P and ϵ_P.

Standard values of the LEC's at order $O(p^4)$ can be found in ref. [3], and were derived with the supposition that the ZR violating LEC's $L_6(\mu)$ and $L_4(\mu)$ were suppressed at the scale $\mu = M_\eta$. The following values have been obtained: $L_4(M_\rho) \cdot 10^3 = -0.3 \pm 0.5$, $L_5(M_\rho) \cdot 10^3 = 1.4 \pm 0.5$, $L_6(M_\rho) \cdot 10^3 = -0.2 \pm 0.3$, $L_7(M_\rho) \cdot 10^3 = -0.4 \pm 0.2$, $L_8(M_\rho) \cdot 10^3 = 0.9 \pm 0.3$. These values are compatible with our analysis: it can be seen on the first lines of table 2, with $L_6(M_\rho) \sim -0.2 \cdot 10^{-3}$, $X(2) \sim X(3) \sim 0.9$, $r = 25$, $F_0 = 85\,\mathrm{MeV}$. The values of $L_4(M_\rho)$ and $L_6(M_\rho)$ correspond also to the lower bounds derived from the saturation of the paramagnetic inequalities for F^2 and X: $X(2) = X(3)$ and $F(2) = F(3)$.

We see that L_4 is weakly sensitive to L_6, in agreement with eqs. (3.4) and (3.7). For large r, and F_0 close to F_π, $1 - \tilde{\eta}(r) - F_0^2/F_\pi^2$ is nearly vanishing, so that L_4 is mainly fixed by the last term in eq. (3.7) with no dependence on $X(3)$. On the contrary, L_5 is clearly dependent on the value of L_6. We can look at eq. (3.6) to understand this phenomenon: $\tilde{\eta}(r)$ may be small, but it never vanishes. The first term in eq. (3.6) leads therefore to large values of L_5 when $X(3)$ decreases, whatever values we choose for r and F_0 (this is related to the definition of L_5). The Gell-Mann–Okubo formula eq. (2.14) correlates strongly L_7 and L_8, leading to $L_7 \simeq -L_8/2$.

From this analysis of the pseudoscalar masses and decay constants, we cannot conclude whether $\bar{q}q$ fluctuations have important effects on the chiral structure of QCD vacuum. However, the values of LEC's are extremely sensitive to the value of $L_6(M_\rho)$. A small shift of L_6 towards positive values would immediately split $X(2)$ and $X(3)$, and increase strongly $L_8(M_\rho)$ and $L_5(M_\rho)$. We will now use additional information from experimental data in the scalar sector, in order to constrain $L_6(M_\rho)$.

5. Sum rule for $X(2) - X(3)$

5.1 Correlator of two scalar densities

We introduce the correlator [17, 18]:

$$\Pi(p^2) = i\frac{mm_s}{M_\pi^2 M_K^2} \lim_{m\to 0} \int d^4x\, e^{ip\cdot x}\, \langle 0|T\{\bar{u}u(x)\ \bar{s}s(0)\}|0\rangle\,, \tag{5.1}$$

that is invariant under the QCD renormalization group, and violates the Zweig rule in the 0^{++} channel. For $m_s \neq 0$, Π is a $\mathrm{SU}_L(2) \otimes \mathrm{SU}_R(2)$ order parameter, related to the derivative of $\Sigma(2)$ with respect to m_s: $mm_s \partial\Sigma(2)/\partial m_s = M_\pi^2 M_K^2 \Pi(0)$.

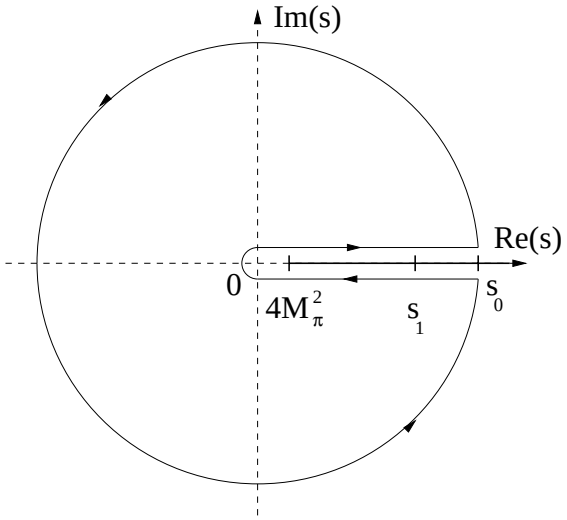

Figure 4: Contour of the integral in the sum rule for the correlator $\langle \bar{u}u\,\bar{s}s\rangle$.

We can use the relation eq. (2.17) between r, $X(3)$ and $X(2)$ to compute $\partial\Sigma(2)/\partial m_s$. Eq. (2.3) can be used to compute $(\partial Z^S/\partial m_s)_{m=0}$. This leads to an equation involving Z^S and $\Pi(0)$:

$$\begin{aligned} X(2)-X(3) &= \frac{2mm_s}{F_\pi^2 M_\pi^2}\, Z^S\Big|_{m=0} + \frac{m}{F_\pi^2 M_\pi^2}\lim_{m\to 0}\frac{F_\pi^2\delta_\pi}{m} \\ &= \frac{2M_K^2}{F_\pi^2}\Pi(0) + \frac{r[X(3)]^2}{32\pi^2}\frac{F_\pi^2 M_\pi^2}{F_0^4}\left(\bar{\lambda}_K + \frac{2}{9}\bar{\lambda}_\eta\right) + \\ &\quad + \frac{m}{F_\pi^2 M_\pi^2}\left(1 - m_s\frac{\partial}{\partial m_s}\right)\lim_{m\to 0}\frac{F_\pi^2\delta_\pi}{m}\,, \end{aligned} \tag{5.2}$$

with the logarithmic derivatives: $\bar{\lambda}_P = m_s\cdot\partial(\log \bar{M}_P^2)/\partial m_s$. This equation contains the NNLO remainder $F_\pi^2\delta_\pi$ in the quark mass expansion of $F_\pi^2 M_\pi^2$. Its leading term is $O(mm_s^2)$, so that the last term in eq. (5.2) should be of order $\sim(-\delta_\pi/M_\pi^2)$.

L_6 (or the difference $X(2)-X(3)$) measures the violation of the Zweig rule in the scalar channel. We are going to exploit experimental information about this violation and to evaluate $\Pi(0)$ through the sum rule:

$$\begin{aligned} \Pi(0) &= \frac{1}{\pi}\int_0^{s_1} ds\,\mathrm{Im}\,\Pi(s)\,\frac{1}{s}\left(1-\frac{s}{s_0}\right) + \\ &\quad + \frac{1}{\pi}\int_{s_1}^{s_0} ds\,\mathrm{Im}\,\Pi(s)\,\frac{1}{s}\left(1-\frac{s}{s_0}\right) + \frac{1}{2i\pi}\int_{|s|=s_0} ds\;\Pi(s)\,\frac{1}{s}\left(1-\frac{s}{s_0}\right). \end{aligned} \tag{5.3}$$

The three terms will be estimated in different ways:

- For $0 \le \sqrt{s} \le \sqrt{s_1} \sim 1.2\,\mathrm{GeV}$, the spectral function $\mathrm{Im}\,\Pi$ is obtained by solving Omnès-Muskhelishvili equations for two coupled channels, using several T-matrix models in the scalar sector.

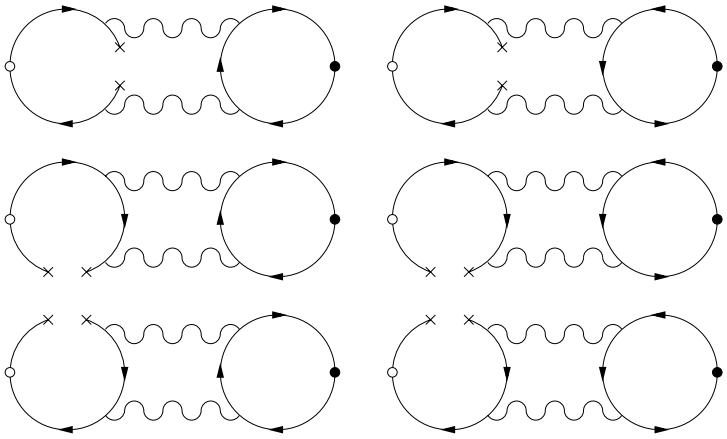

Figure 5: Feynman diagrams contributing to $m_s\langle\bar{u}u\rangle$ in OPE of Π (lowest order in α_s). The white circle is the scalar source $\bar{u}u$, the black one $\bar{s}s$.

- For $\sqrt{s_1} \leq \sqrt{s} \leq \sqrt{s_0} \sim 1.5\,\mathrm{GeV}$, the spectral function under s_1 is exploited through another sum rule in order to bound the contribution of the integral.
- For $|s| = s_0$, we estimate the integral through Operator Product Expansion (OPE).

5.2 Asymptotic behavior

Π can be expanded using OPE:

$$\begin{aligned}\Pi(p^2) &= i\frac{mm_s}{M_\pi^2 M_K^2}\lim_{m\to 0}\int d^4x\, e^{ip\cdot x}\,\langle 0|T[\bar{u}u(x)\,\bar{s}s(0)]|0\rangle \\ &\underset{P^2\to\infty}{\sim} \frac{mm_s}{M_\pi^2 M_K^2}\sum_{n\geq 4}\frac{1}{(P^2)^{n/2-1}}C^{(n)}(t)\langle 0|\mathcal{O}_n|0\rangle, \end{aligned} \tag{5.4}$$

with $P^2 = -p^2$, μ a renormalization scale, $t = \mu^2/P^2$, and $\mathcal{O}_n$ a combination of n-dimensional operators. Π transforms chirally as $(\bar{u}u)(\bar{s}s)$ and we take the chiral limit $m \to 0$. Hence, the lowest-dimension operator is $\mathcal{O}_4 = m_s\bar{u}u$, and the contributing diagrams include at least two gluonic lines [17].

We will work in dimensional regularization ($d = 4-2\omega$). In the class of t'Hooft's gauges, the gluon propagator reads:

$$\frac{-i}{k^2+i\epsilon}\left(g_{\mu\nu} - (1-\xi)\frac{k_\mu k_\nu}{k^2+i\epsilon}\right)\delta_{ab}\,, \tag{5.5}$$

with ξ a free real parameter. The Wilson coefficient of $m_s\bar{u}u$ (at the leading order) is obtained by adding 6 two-loop integrals. It is easy to see that the contributions of ξ and ξ^2 cancel in this sum of integrals. Hence, we check that the Wilson coefficient of $m_s\bar{u}u$ at the leading order is independent of the chosen gauge, in the class of t'Hooft's gauges.

We want the large-P^2 limit of integrals like:

$$g_s^4\mu^{4\omega}m_s\langle\bar{u}u\rangle\frac{1}{p^2}\int\frac{d^4q}{(2\pi)^d}\frac{d^4k}{(2\pi)^d}\mathcal{P}(p^2,q^2,k^2,p\cdot q,p\cdot k,q\cdot k,m_s^2)\times$$
$$\times\frac{1}{[(p-q)^2-m_0^2]^{n_2}[q^2-m_0^2]^{n_3}}\times$$
$$\times\frac{1}{[(k+p)^2-m_s^2]^{n_4}[(k+q)^2-m_s^2]^{n_5}[k^2-m_s^2]^{n_6}}\,, \tag{5.6}$$

where $\mathcal{P}$ is a polynomial of degree 2. m_0 corresponds at the same time to $m=m_u=m_d$ for fermion propagators in the loop of $u-d$ quarks, and to a fictitious mass to regularize infrared gluonic divergences (we take at the end the limit $m_0\to 0$).

Using identities like $2(k\cdot q)=[(k+q)^2+m_s^2]-[k^2+m_s^2]-q^2$, we can reexpress the sum in terms of:

$$\frac{1}{p^{2\nu_0}}J(\{\nu_i\},\{m_i\},p)=\frac{1}{p^{2\nu_0}}\int\frac{d^4q\;d^4k}{[q^2-m_0^2]^{\nu_1}[k^2-m_s^2]^{\nu_2}}\times$$
$$\times\frac{1}{[(k+q)^2-m_s^2]^{\nu_3}[(p-q)^2-m_0^2]^{\nu_4}[(k+p)^2-m_s^2]^{\nu_5}}\,, \tag{5.7}$$

with $m_1=m_4=m_0$ and $m_2=m_3=m_5=m_s$. These integrals are formally identical to the ones arising for two-loop self-energies. The behavior of such integrals at large external momentum has already been studied. The basic idea consists in following the flow of the large external momentum through the Feynman diagrams, in order to Taylor expand the propagators [24]. This procedure, based on the asymptotic expansion theorem [25], is sketched in appendix B.

Rather lengthy computations lead to the first term arising in the OPE of the correlator. Some integrals contain poles in $1/\omega$, but these divergences cancel when all the contributions are summed (this cancellation is a non-trivial check of the procedure). The first term in OPE is:

$$i\frac{mm_s}{M_\pi^2M_K^2}\lim_{m\to 0}\int d^4x\,e^{ip\cdot x}\,\langle 0|T\{m\bar{u}u(x)\;m_s\bar{s}s(0)\}|0\rangle\underset{P^2\to\infty}{\sim}$$
$$\underset{P^2\to\infty}{\sim}-\frac{18[1-2\zeta(3)]}{P^2}\left(\frac{\alpha_s}{\pi}\right)^2\frac{m_s^2}{M_\pi^2M_K^2}m\langle\bar{u}u\rangle\,. \tag{5.8}$$

The involved condensate should be the two-flavor one ($m\to 0$, $m_s\neq 0$).

5.3 Contribution for $s\leq s_1$: pion and kaon scalar form factors

5.3.1 Omnès-Muskhelishvili equations

In order to compute the integral:

$$\mathcal{I}=\frac{1}{\pi}\int_0^{s_1}ds\,\mathrm{Im}\,\Pi(s)\,\frac{1}{s}\left(1-\frac{s}{s_0}\right), \tag{5.9}$$

we have to know Im Π between 0 and s_1 ($\sqrt{s}_1 \sim 1.2\,\mathrm{GeV}$). The procedure is explained in detail in refs. [17, 18], and we shall merely sketch its main features for completeness. In the range of energy between 0 and s_1, the $\pi\pi$- and $K\bar{K}$- channels should dominate the spectral function [17, 26, 27]. If we denote these channels respectively 1 and 2, the spectral function is:

$$\mathrm{Im}\,\Pi(s) = \frac{mm_s}{M_\pi^2 M_K^2}\frac{1}{16\pi}\sum_{i=1,2}\sqrt{\frac{s-4M_i^2}{s}}[n_i F_i(s)][n_i G_i^*(s)]\theta(s-4M_i^2)\,, \tag{5.10}$$

with the scalar form factors for the pion and the kaon:

$$\vec{F}(s) = \begin{pmatrix}\langle 0|\bar{u}u|\pi\pi\rangle \\ \langle 0|\bar{u}u|K\bar{K}\rangle\end{pmatrix}, \qquad \vec{G}(s) = \begin{pmatrix}\langle 0|\bar{s}s|\pi\pi\rangle \\ \langle 0|\bar{s}s|K\bar{K}\rangle\end{pmatrix}, \tag{5.11}$$

with $M_1 = M_\pi$ and $M_2 = M_K$. $n_1 = \sqrt{3/2}$ and $n_2 = \sqrt{2}$ are numerical factors related to the normalization of the states $|\pi\pi\rangle$ and $|K\bar{K}\rangle$.

The form factors are analytic functions in the complex plane, with the exception of a right cut along the real axis. They should have the asymptotic behavior $F_i(s) \sim 1/s$ when $s \to \infty$, and fulfill a dispersion relation with no subtraction. Obviously, when s increases, new channels open, and the two-channel approximation is no more sufficient. But we need $\vec{F}$ and $\vec{G}$ for $s \leq s_1$, and we are not interested in the behavior of the spectral function at much higher energies. We can therefore suppose that the two-channel approximation is valid for any energies, with the discontinuity along the cut:

$$S_{ij} = \delta_{ij} + 2i\sigma_i^{1/2} T_{ij}\sigma_j^{1/2}\theta(s-4M_i^2)\theta(s-4M_j^2)\,, \tag{5.12}$$

$$\mathrm{Im}\,F_i(s) = \sum_{j=1}^{n} T_{ij}^*(s)\sigma_j(s)F_j(s)\theta(s-4M_j^2)\,, \qquad \sigma_i = \sqrt{\frac{s-4M_i^2}{s}}\,, \tag{5.13}$$

and we will suppose in addition that the two-channel T-matrix model impose the correct asymptotic behavior for $\vec{F}$ and $\vec{G}$.

Under these assumptions, $\vec{F}$ and $\vec{G}$ satisfy separately a set of coupled Omnès-Muskhelishvili equations [17, 26, 28, 29]:

$$F_i(s) = \frac{1}{\pi}\sum_{j=1}^{n}\int_{4M_\pi^2}^{\infty} ds' \frac{1}{s'-s}T_{ij}^*(s')\sqrt{\frac{s'-4M_j^2}{s'}}\theta(s'-4M_j^2)F_j(s')\,, \tag{5.14}$$

with the condition that the T matrix leads to the expected decrease of the form factors for $s \to \infty$. Ref. [17] has proved a condition of existence and unicity for the solution of eq. (5.14): $\Delta(\infty) - \Delta(4M_\pi^2) = 2\pi$, where $\Delta(s)$ is the sum of the $\pi\pi$ and $K\bar{K}$ phase shifts. In that case, the set of linear equations admits a unique solution, once the values at a given energy are fixed [18]. All the solutions are thus

linear combinations of a basis, for instance the solutions $\vec{A}(s)$ and $\vec{B}(s)$ such as: $\vec{A}(0) = \binom{1}{0}$ and $\vec{B}(0) = \binom{0}{1}$. $\vec{F}$ and $\vec{G}$ can therefore be written as:

$$\vec{F}(s) = F_1(0)\vec{A}(s) + F_2(0)\vec{B}(s)\,, \qquad \vec{G}(s) = G_1(0)\vec{A}(s) + G_2(0)\vec{B}(s)\,. \tag{5.15}$$

The value of the form factors at zero is related to the derivatives of the pseudoscalar masses with respect to the quark masses:

$$\begin{aligned} F_1(0) &= \frac{1}{2}\left(\frac{\partial M_\pi^2}{\partial m}\right)_{m=0}\,, & F_2(0) &= \frac{1}{2}\left(\frac{\partial M_K^2}{\partial m}\right)_{m=0}\,, \\ G_1(0) &= \left(\frac{\partial M_\pi^2}{\partial m_s}\right)_{m=0} = 0\,, & G_2(0) &= \left(\frac{\partial M_K^2}{\partial m_s}\right)_{m=0}\,. \end{aligned} \tag{5.16}$$

Up to now, we have followed the same line as refs. [17, 26]. But in these papers, the value of the scalar form factors at zero was derived using Standard χPT, i.e. supposing that the three-flavor quark condensate dominates the expansion of the pseudoscalar masses. We are going to allow a competition between the terms linear and quadratic in quark masses, so that the normalization of the form factors may become rather different from what is considered in refs. [17, 26]. In a similar way, the form factors that we will obtain could differ from the ones obtained by a matching with Standard one-loop expressions [27, 30].

We consider here three models of T-matrix, proposed respectively by Oller, Oset and Pelaez in ref. [31], by Au, Morgan and Pennington in ref. [32], and by Kaminski, Lesniak and Maillet in ref. [33]. These models fit correctly the available data in the scalar sector under 1.3 GeV, as discussed in refs. [17, 26, 31]. However, they have to be corrected for very low and very high energies, as discussed in ref. [17]: chiral symmetry constrains the $\pi\pi$ phase shift near the threshold, and the asymptotic behavior of the phases shifts has to be changed to insure existence and unicity for the solution of eq. (5.14).

5.3.2 Contribution of the first integral

If we put eq. (5.15) into eq. (5.10), we obtain the spectral function as the sum of two contributions:

$$\begin{aligned} \mathrm{Im}\,\Pi(s) = {} & \gamma_\pi\lambda_K\left[\frac{\sqrt{3}}{32\pi}\sum_{i=1,2}\sqrt{\frac{s-4M_i^2}{s}}A_i(s)B_i^*(s)\theta(s-4M_i^2)\right] + \\ & + \gamma_K\lambda_K\frac{M_K^2}{M_\pi^2}\left[\frac{1}{16\pi}\sum_{i=1,2}\sqrt{\frac{s-4M_i^2}{s}}B_i(s)B_i^*(s)\theta(s-4M_i^2)\right], \end{aligned} \tag{5.17}$$

where the logarithmic derivatives of the masses are denoted:

$$\lambda_P = \frac{m_s}{M_P^2}\left(\frac{\partial M_P^2}{\partial m_s}\right)_{m=0} = \frac{m_s}{M_P^2}\frac{\partial \bar{M}_P^2}{\partial m_s}, \qquad \gamma_P = \frac{m}{M_P^2}\left(\frac{\partial M_P^2}{\partial m}\right)_{m=0}\,. \tag{5.18}$$

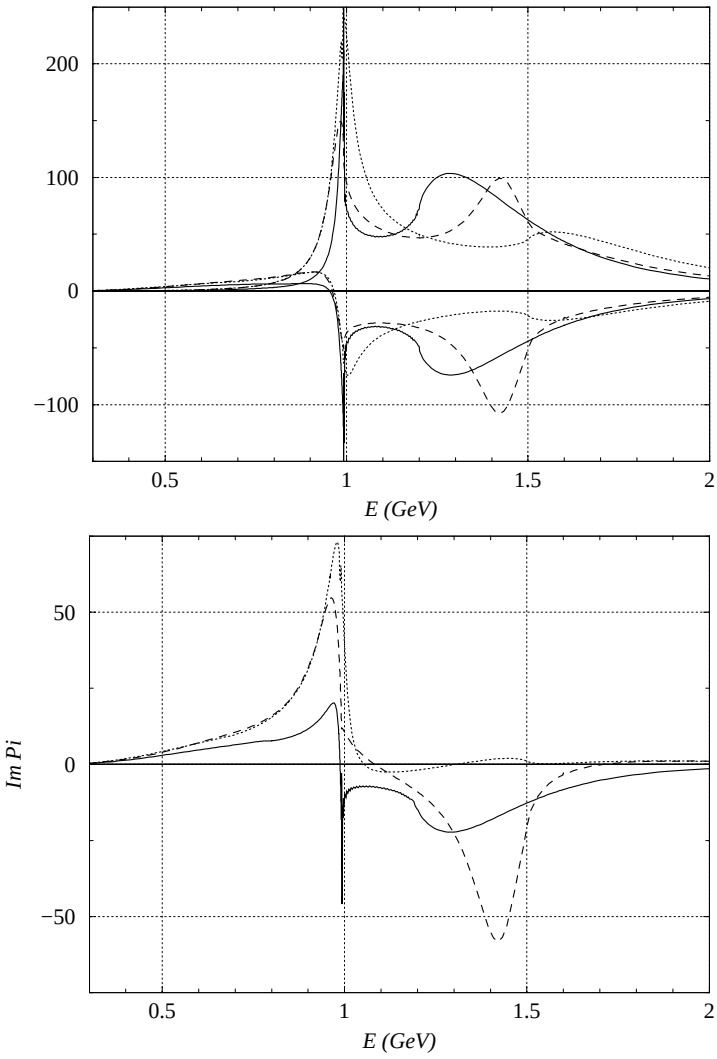

Figure 6: Up: Contributions of type BB^* (positive) and type AB^* (negative) to the spectral function. Down: example of spectral function, obtained with $\gamma_\pi = 1$, $\lambda_K = 1 - M_\pi^2/(2M_K^2)$ and $\gamma_K = M_\pi^2/(2M_K^2)$. In both cases, we plot the results for the T-matrix models of ref. [31] (solid lines), ref. [32] (dotted) and ref. [33] (dashed).

The two bracketed functions in eq. (5.17) can be plotted: the first one is called "type AB^*", the second one "type BB^*". It is also interesting to study how these two contributions cancel each other inside the spectral function, by taking the Standard tree-level estimates: $\gamma_\pi = 1$, $\lambda_K = 1 - M_\pi^2/(2M_K^2)$ and $\gamma_K = M_\pi^2/(2M_K^2)$. A peak, corresponding to the narrow resonance $f_0(980)$ [8], arises with a height depending on the models: ref. [31] leads to a smaller peak than refs. [32] and [33].

The integral between 0 and s_1 in the sum rule eq. (5.3) can be written, using eq. (5.17):

$$\frac{1}{\pi}\int_0^{s_1} ds\, \mathrm{Im}\,\Pi(s)\frac{1}{s}\left(1-\frac{s}{s_0}\right) = \gamma_\pi\lambda_K\mathcal{I}_{AB} + \gamma_K\lambda_K\frac{M_K^2}{M_\pi^2}\mathcal{I}_{BB}\,, \tag{5.19}$$

JHEP03(2001)002

where $\mathcal{I}_{XY} = \mathcal{M}_{XY}^{(-1)} - \mathcal{M}_{XY}^{(0)}/s_0$, involves the moments:

$$\mathcal{M}_{AB}^{(k)} = \frac{\sqrt{3}}{32\pi^2}\int_0^{s_1} ds\, s^k \sum_{i=1,2}\sqrt{\frac{s-4M_i^2}{s}}A_i(s)B_i^*(s)\theta(s-4M_i^2)\,, \tag{5.20}$$

$$\mathcal{M}_{BB}^{(k)} = \frac{1}{16\pi^2}\int_0^{s_1} ds\, s^k \sum_{i=1,2}\sqrt{\frac{s-4M_i^2}{s}}B_i(s)B_i^*(s)\theta(s-4M_i^2)\,. \tag{5.21}$$

Notice that we solve Omnès-Muskhelishvili equations to obtain the scalar form factors of the pion and the kaon in the limit $m \to 0$ (and m_s fixed at its physical value). But we consider T-matrix models fitting experimental data, with up and down quarks with their physical masses. The limit $m \to 0$ sets the $\pi\pi$-threshold to zero,[4] changes $\pi\pi$ phase shifts near the threshold and shifts slightly the $K\bar{K}$ threshold. Such modifications should not alter significantly the general shape of the spectral function. In particular, the integral of the spectral function, dominated by the $f_0(980)$ peak, should be affected only marginally when $T_{\mathrm{m}\neq 0}$ is considered instead of $T_{\mathrm{m}\to 0}$.

5.4 Second sum rule: $s_1 \leq s \leq s_0$

The contribution of the integral below s_1 is positive and dominated by the $f_0(980)$ peak. But according to section 5.2, Π is superconvergent, and the integral of the spectral function from 0 to infinity vanishes. $\mathrm{Im}\,\Pi(s)$ should therefore become negative in some range of energy. In particular, negative peaks should rather naturally appear in the spectral function, in relation with massive scalar resonances like $f_0(1370)$ and $f_0(1500)$ [8].

Let us suppose that the spectral function is negative for $s_1 \leq s \leq s_0$.[5] The contribution from the intermediate region in eq. (5.2) can be estimated from:

$$\frac{1}{s_0}\mathcal{J}' \leq -\frac{1}{\pi}\int_{s_1}^{s_0} ds\,\mathrm{Im}\,\Pi(s)\,\frac{1}{s}\left(1-\frac{s}{s_0}\right) \leq \frac{1}{s_1}\mathcal{J}'\,, \tag{5.23}$$

where $\mathcal{J}'$ is the integral:

$$\mathcal{J}' = \frac{1}{\pi}\int_{s_1}^{s_0} ds\,\mathrm{Im}\,\Pi(s)\left(1-\frac{s}{s_0}\right), \tag{5.24}$$

[4] For $m \to 0$, the cut along the real axis starts at $s = 0$. However, the integral $\int_0^{s_0} ds\,(1-s/s_0)\cdot \mathrm{Im}\,\Pi(s)/s$ is convergent, since for $s \to 0$: $F_1(s) \to F_1(0)$ and $G_1(s) \sim G_1'(0)\cdot s$, leading to:

$$\mathrm{Im}\,\Pi(s) \sim \frac{3}{32\pi}\frac{m m_s}{M_\pi^2 M_K^2}F_1(0)G_1'(0)\cdot s\,. \tag{5.22}$$

[5] If the spectral function is partially positive in this range, our hypothesis will end up with an estimate for the second integral that will be smaller than its actual value. In that case, we would underestimate the difference $X(2) - X(3)$.

which satisfies the sum rule:

$$\frac{1}{\pi}\int_0^{s_1} ds\,\mathrm{Im}\,\Pi(s)\left(1-\frac{s}{s_0}\right)+\mathcal{J}'+\frac{1}{2i\pi}\int_{|s|=s_0} ds\,\Pi(s)\left(1-\frac{s}{s_0}\right)=0\,. \tag{5.25}$$

The first integral in eq. (5.25) can be computed from the spectral function obtained in the previous section:

$$\frac{1}{\pi}\int_0^{s_1} ds\,\mathrm{Im}\,\Pi(s)\left(1-\frac{s}{s_0}\right)=\gamma_\pi\lambda_K\mathcal{I}'_{AB}+\gamma_K\lambda_K\frac{M_K^2}{M_\pi^2}\mathcal{I}'_{BB}\,, \tag{5.26}$$

with $\mathcal{I}'_{XY}=\mathcal{M}^{(0)}_{XY}-\mathcal{M}^{(1)}_{XY}/s_0$ involving the moments eqs. (5.20)–(5.21).

The contribution from the complex circle (third integral in eq. (5.25)) can be estimated through Operator Product Expansion (OPE), using the method described in the following section:

$$\begin{aligned}\frac{1}{2i\pi}\int_{|s|=s_0} ds\,\Pi(s)\left(1-\frac{s}{s_0}\right) &= 9[1-2\zeta(3)]\frac{F_\pi^2}{M_K^2}X(2)m_s^2(s_0)a^2(s_0)\times\\ &\quad\times\left\{1+\frac{\beta_0\gamma}{2}a(s_0)+\right.\\ &\quad\left.+\left[\frac{\beta_1\gamma}{2}-\frac{\gamma(\gamma+1)}{8}\left(\frac{\pi^2}{3}-2\right)\beta_0^2\right]a^2(s_0)\right\}+\cdots\\ &= 9[1-2\zeta(3)]\frac{F_\pi^2}{M_K^2}X(2)m_s^2(s_0)a^2(s_0)\times\\ &\quad\times\left[1+6.5\cdot a(s_0)-25.125\cdot a^2(s_0)\right].\end{aligned} \tag{5.27}$$

5.5 High-energy contribution: $|s|=s_0$

We want the contribution of the integral on the large circle:

$$\mathcal{K}=\frac{1}{2i\pi}\int_{|s|=s_0} ds\,\Pi(s)\frac{1}{s}\left(1-\frac{s}{s_0}\right)=\frac{1}{2\pi}\int_{-\pi}^{\pi} d\theta\,(1+e^{i\theta})\,\Pi(p^2=-s_0e^{i\theta})\,. \tag{5.28}$$

The factor $(1-s/s_0)$ suppresses the contribution stemming from the time-like region around s_0, so that we can use in this integral the Operator Product Expansion of Π [34]. Once Renormalization Group Improvement is applied to eq. (5.8), the QCD renormalization group invariant $m\langle\bar{u}u\rangle$ gets the coefficient:

$$a^2(P^2)m_s^2(P^2)=a^2(s_0)m_s^2(s_0)\times\left[\frac{a(P^2)}{a(s_0)}\right]^{8/b_0+2}, \tag{5.29}$$

with $a(s)=\alpha_s(s)/\pi$ and $b_0=11-2N_f/3=9$. The integral eq. (5.28) becomes:

$$\mathcal{K}=\frac{9[1-2\zeta(3)]}{2\pi}\frac{F_\pi^2}{M_K^2}X(2)\frac{m_s^2(s_0)}{s_0}[a(s_0)]^{-8/b_0}\int_{-\pi}^{\pi} ds\,(1+e^{-i\theta})\,a^\gamma(s_0e^{i\theta})\,, \tag{5.30}$$

with $\gamma = 2 + 8/b_0 = 2 + 8/9$. To compute this integral, we expand $a(P^2 = s_0 e^{i\theta})$ in powers of $a(s_0)$. The behavior of $a(t)$ (t complex) depends on the β function:

$$t\frac{d}{dt}a(t) = \frac{1}{2\pi}\beta[a(t)], \qquad \frac{1}{\pi}\beta[a(t)] = -\beta_0 a^2 - \beta_1 a^3 + \cdots,$$
$$\beta_0 = \frac{33 - 2N_f}{6} = \frac{9}{2}, \qquad \beta_1 = \frac{306 - 38N_f}{24} = 8\,. \tag{5.31}$$

The expansion of $a(s_0 e^{i\theta})$ is:

$$a(s_0 e^{i\theta}) = a(s_0) - \frac{i}{2}\beta_0\theta a^2(s_0) + \left[\frac{i}{2}\beta_1\theta - \frac{1}{4}\theta\beta_0^2\theta^2\right] a^3(s_0) + O(a^4)\,. \tag{5.32}$$

We get:

$$\begin{aligned}\mathcal{K} &= 9[1 - 2\zeta(3)]\frac{F_\pi^2}{M_K^2}X(2)\frac{m_s^2(s_0)}{s_0}a^2(s_0) \times \\ &\quad \times \left\{1 - \frac{\beta_0\gamma}{2}a(s_0) - \left[\frac{\beta_1\gamma}{2} + \frac{\gamma(\gamma+1)}{8}\left(\frac{\pi^2}{3} - 2\right)\beta_0^2\right] a^2(s_0)\right\} + \cdots \\ &= 9[1 - 2\zeta(3)]\frac{F_\pi^2}{M_K^2}X(2)\frac{m_s^2(s_0)}{s_0}a^2(s_0)[1 - 6.5 \cdot a(s_0) + 48.236 \cdot a^2(s_0)]\,.\end{aligned} \tag{5.33}$$

This negative contribution is strongly suppressed by α_s^2 and m_s^2/s_0. We have considered here $m_s \sim 200\,\mathrm{MeV}$, but the contribution of this integral is so small that the error due to m_s and α_s can be neglected. Notice that duality is not supposed to arise in the scalar sector for as low energies as in other channels, due to a probably large contribution from the direct instantons in this sector [35].

6. Results

6.1 Logarithmic derivatives of pseudoscalar masses

The logarithmic derivatives of the masses are obtained from the expansions of F_P^2 and $F_P^2 M_P^2$:

$$\lambda_P = \frac{m_s}{M_P^2}\left(\frac{\partial M_P^2}{\partial m_s}\right)_{m=0} = \frac{m_s}{M_P^2}\frac{\partial \bar{M}_P^2}{\partial m_s}\,, \qquad \gamma_P = \frac{m}{M_P^2}\left(\frac{\partial M_P^2}{\partial m}\right)_{m=0}\,. \tag{6.1}$$

The corresponding expressions are given in appendix C.1. We have $\lambda_\pi = 0$ since it is proportional to the derivative of M_π^2 with respect to m_s in the limit $m \to 0$.

We would obtain at the one-loop order in the Standard framework:

$$\gamma_\pi \sim 1\,, \qquad \gamma_K \sim \frac{M_\pi^2}{2M_K^2} = 0.04\,, \qquad \gamma_\eta \sim \frac{M_\pi^2}{3M_\eta^2} = 0.02\,, \tag{6.2}$$

$$\lambda_K \sim 1 - \frac{M_\pi^2}{2M_K^2} = 0.96\,, \qquad \lambda_\eta \sim \frac{4M_K^2}{3M_\eta^2} = 1.09\,. \tag{6.3}$$

	$r=20$			$r=25$			$r=30$		
$X(3)$	γ_π	γ_K	γ_η	γ_π	γ_K	γ_η	γ_π	γ_K	γ_η
0.	0.876	0.090	0.081	0.930	0.078	0.068	0.958	0.070	0.059
0.3	0.920	0.082	0.071	0.970	0.069	0.058	0.995	0.060	0.049
0.5	0.946	0.074	0.062	0.992	0.060	0.048	1.015	0.051	0.038
0.7	0.967	0.064	0.052	1.009	0.050	0.036	1.029	0.039	0.025
0.8	0.975	0.059	0.046	1.016	0.044	0.030	1.034	0.033	0.019
0.9	-	-	-	1.021	0.038	0.024	1.038	0.027	0.013
0.	0.892	0.080	0.072	0.943	0.070	0.060	0.970	0.063	0.053
0.3	0.941	0.072	0.062	0.990	0.061	0.050	1.011	0.053	0.041
0.5	0.965	0.063	0.051	1.009	0.051	0.038	1.029	0.042	0.029
0.7	0.980	0.052	0.039	1.020	0.038	0.025	1.037	0.029	0.015
0.8	0.983	0.046	0.032	1.022	0.032	0.018	1.037	0.022	0.009

Table 3: Logarithmic derivatives with respect to m: γ_π, γ_K and γ_η, as functions of $X(3)$ and r, for $F_0 = 85\,\mathrm{MeV}$ (upper part) and $F_0 = 75\,\mathrm{MeV}$ (lower part).

	$r=20$		$r=25$		$r=30$	
$X(3)$	λ_K	λ_η	λ_K	λ_η	λ_K	λ_η
0.	1.438	1.398	1.455	1.416	1.467	1.428
0.3	1.391	1.346	1.383	1.339	1.366	1.321
0.5	1.326	1.276	1.284	1.231	1.226	1.169
0.7	1.236	1.179	1.148	1.086	1.041	0.975
0.8	1.183	1.123	1.070	1.005	0.938	0.871
0.9	-	-	0.986	0.921	0.833	0.768
0.	1.341	1.310	1.354	1.323	1.362	1.332
0.3	1.302	1.263	1.287	1.247	1.261	1.220
0.5	1.224	1.177	1.163	1.111	1.086	1.029
0.7	1.109	1.053	0.991	0.931	0.858	0.796
0.8	1.041	0.982	0.894	0.834	0.739	0.681

Table 4: Logarithmic derivatives with respect to m_s: λ_K and λ_η, as functions of r and $X(3)$, for $F_0 = 85\,\mathrm{MeV}$ (upper part) and $F_0 = 75\,\mathrm{MeV}$ (lower part).

The logarithmic derivatives differ from these values because of the terms quadratic in the quark masses in the expansions of $F_P^2 M_P^2$. The tables 3 and 4 collect values of these derivatives for $r = 20, 25, 30$, and $F_0 = 75\,\mathrm{MeV}$ and $85\,\mathrm{MeV}$. We note that the values for $F_0 = 85\,\mathrm{MeV}$, $r = 25$, $X(3) \sim 0.8$ are in correct agreement with the Standard tree-level estimates eqs. (6.2)–(6.3).

We can notice that γ_π remains close to 1 if we change F_0, r and $X(3)$. γ_π involves the linear m-dependence of the pion mass, which can be written as: $F_\pi^2 M_\pi^2 = 2m\Sigma(2) + O(m^2)$. Therefore, γ_π is related to the two-flavor quark condensate $\Sigma(2)$,

which is very weakly dependent on the values of F_0 and $X(3)$ (it is affected by the value of r, but our tables show only large values of r where $X(2)$ does not strongly vary). On the other hand, γ_K and γ_η are rather sensitive to $X(3)$. These two logarithmic derivatives are $1/r$-suppressed when the three-flavor quark condensate is large. If $X(3)$ decreases, these 2 quantities feel strongly the presence of large higher-order contributions.

λ_K and λ_η increase from 1 to 1.4 when $X(3)$ decreases down to 0. If $X(3)$ vanishes, the pseudoscalar masses are dominated by terms quadratic in m_s. In that case, we would naively expect logarithmic derivatives to be twice as large as for $X(3) \sim 1$. To understand this discrepancy, it is useful to consider the second kind of logarithmic derivatives arising in eq. (5.2):

$$\bar{\lambda}_P = \frac{m_s}{\bar{M}_P^2}\frac{\partial \bar{M}_P^2}{\partial m_s} = \frac{M_P^2}{\bar{M}_P^2}\lambda_P\,, \qquad P = K, \eta \tag{6.4}$$

λ_P and $\bar{\lambda}_P$ are related, but the first is suppressed with respect to the latter by a factor $\bar{M}_P^2/M_P^2$. For instance, in the limit of a vanishing three-flavor condensate, the expansion of $\bar{F}_P^2\bar{M}_P^2$ begins with terms quadratic in m_s, so that $\bar{\lambda}_P$ is of order 2, whereas $\lambda_P = \bar{\lambda}_P \cdot \bar{M}_P^2/M_P^2$ is suppressed, and reaches lower values around 1.4–1.5.

To obtain the values of tables 3 and 4, we had to neglect the remainders of higher order ϵ_P and δ_P. It is difficult to estimate the size of the resulting errors for the logarithmic derivatives γ_P and λ_P. Suppose for instance that ϵ_P/F_P^2 and δ_P/M_P^2 are smaller than 10 %. To know the impact on γ_P and λ_P, we would have to calculate the values of the derivatives of ϵ_P and δ_P with respect to m and m_s. If we know only the size of ϵ_P/F_P^2 and δ_P/M_P^2, it is hard to get any information about their derivatives, and to estimate the resulting errors on the logarithmic derivatives of the pseudoscalar masses.

6.2 Estimate of $X(3)$ and of LEC's

Hence, two different estimates of $X(2)-X(3)$ are available: the first one is the relation between $X(2)$ and $X(3)$ (eq. (2.17)), the second one consists of the relation between $X(2)-X(3)$ and $\Pi(0)$ (eq. (5.2)) and the sum rule for $\Pi(0)$ (eq. (5.3)). In both cases, the difference $X(2) - X(3)$ can be expressed as a function of the observables and of $F_0, r, X(3)$. This overdertermination can be viewed as a constraint fixing $X(3)$ in terms of r and F_0, see figures 7 and 8.

This analysis contains 3 sources of errors.

(i) First, we have neglected NNLO remainders in the expansions of pseudoscalar masses and decay constants. Their effect is easy to control in the relations between $X(2)$ and $X(3)$ (eq. (2.17)) or $F(2)$ and $F(3)$ (eq. (3.15)), but the situation gets more complicated for the sum rule eq. (5.2) and for the logarithmic derivatives λ_P and γ_P. In the framework of Standard χPT, the authors of ref. [6]

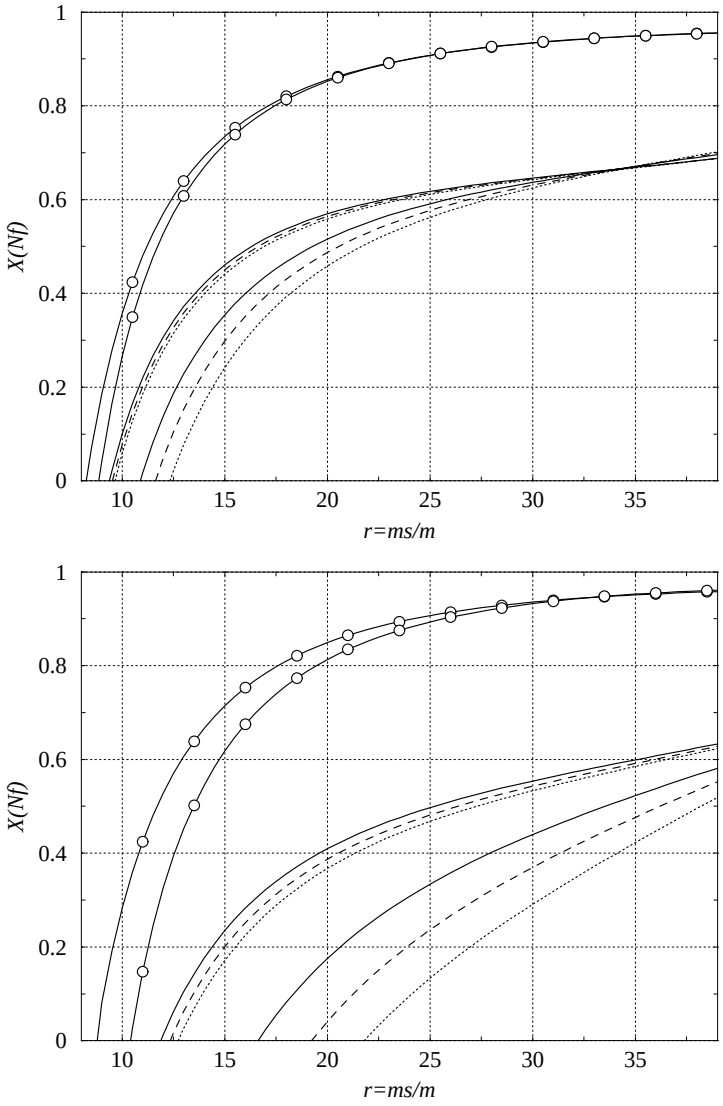

Figure 7: Sum rule: range for $X(3)$ as a function of $r = m_s/m$ for $F_0 = 85\,\mathrm{MeV}$, with the T-matrix models of refs. [31] (up) and [32] (down). The results are plotted for $s_1 = 1.2\,\mathrm{GeV}$ and $s_0 = 1.5\,\mathrm{GeV}$ (solid lines), $1.6\,\mathrm{GeV}$ (dashed lines) and $1.7\,\mathrm{GeV}$ (dotted lines). The lines with white circles show the corresponding range for $X(2)$.

noticed that the dependence on m_s of $\Sigma(2)$ is not really affected by two-loop effects. In addition, these effects have the same sign as one-loop contributions: if they were significant, they would increase (and not decrease) the gap between $X(2)$ and $X(3)$. A similar conclusion was drawn in ref. [18]. The NNLO remainders are supposed here to be small, and they are not included in the results.

(ii) The evaluation of the sum rule eq. (5.3) relies on an estimate of the integral between s_1 and s_0. If we choose a couple (F_0, r), we will not end up with one value for $X(3)$, but rather a range of acceptable values that will also depend

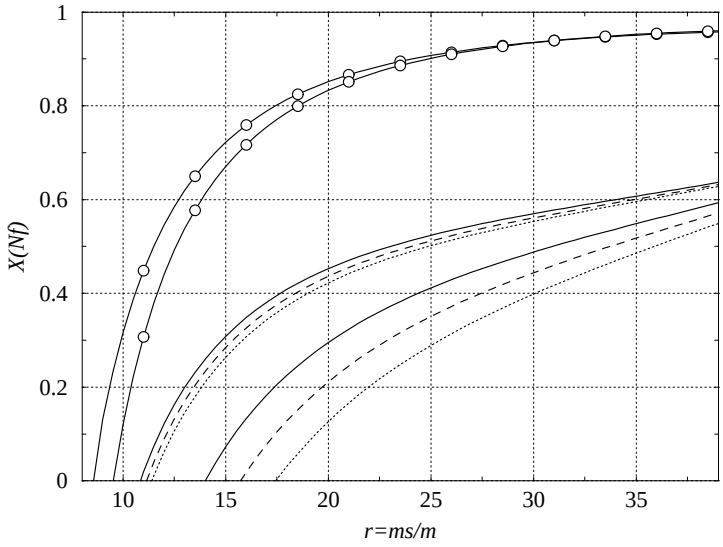

Figure 8: Sum rule: range for $X(3)$ as a function of $r = m_s/m$ for $F_0 = 85\,\mathrm{MeV}$, with the T-matrix models of ref. [33]. The results are plotted for $s_1 = 1.2\,\mathrm{GeV}$ and $s_0 = 1.5\,\mathrm{GeV}$ (solid lines), 1.6 GeV (dashed lines) and 1.7 GeV (dotted lines). The lines with white circles show the corresponding range for $X(2)$.

on the separators $s_1 < s_0$. On the figures 7 and 8, the upper bound for $X(3)$ remains stable for $\sqrt{s_0} > 1.5\,\mathrm{GeV}$, whereas the lower bound depends strongly on s_0. When s_0 increases, the lower bound of eq. (5.23) is too loose to be saturated. A more stringent lower bound would be welcome.

(iii) The third source of error is the T-matrix used to build the spectral function eq. (5.17) for $s < s_1$. Three different models of T-matrix have been used [32, 33, 31]. The central element is the shape of the $f_0(980)$ peak. Ref. [31] leads to the least pronounced effect. The two other models [32, 33] lead to a higher $f_0(980)$ peak, a larger value for $\Pi(0)$, and a smaller value for $X(3)$.

The range for $X(3)$ is much narrower for large values of r, and can be even reduced to one value in the case of ref. [31]. This range should be broadened if we took into account the errors related to higher orders in the expansion of pseudoscalar masses and decay constants. The value of F_0 has no major influence on the constraint for $[X(3), r]$. For instance, choosing $F_0 = 75\,\mathrm{MeV}$ would slightly shift the curves for $X(3)$ towards the left of the graphs ($r \to r - 2$). Similarly, a change of $\sqrt{s_1}$ around 1.2 GeV does not affect strongly the results. If we choose $\sqrt{s_1} = 1.3\,\mathrm{GeV}$, the convergence of the upper bound is slightly less good, but its values remain very close to figures 7 and 8. We should add a last comment for $r \sim 25$ (commonly used in the Standard framework): the values of $X(3)$ correspond then to the half of $X(2)$. We end up with a similar result to the one obtained in refs. [17, 18], but without relying on the hypothesis $X(3) \sim 1$.

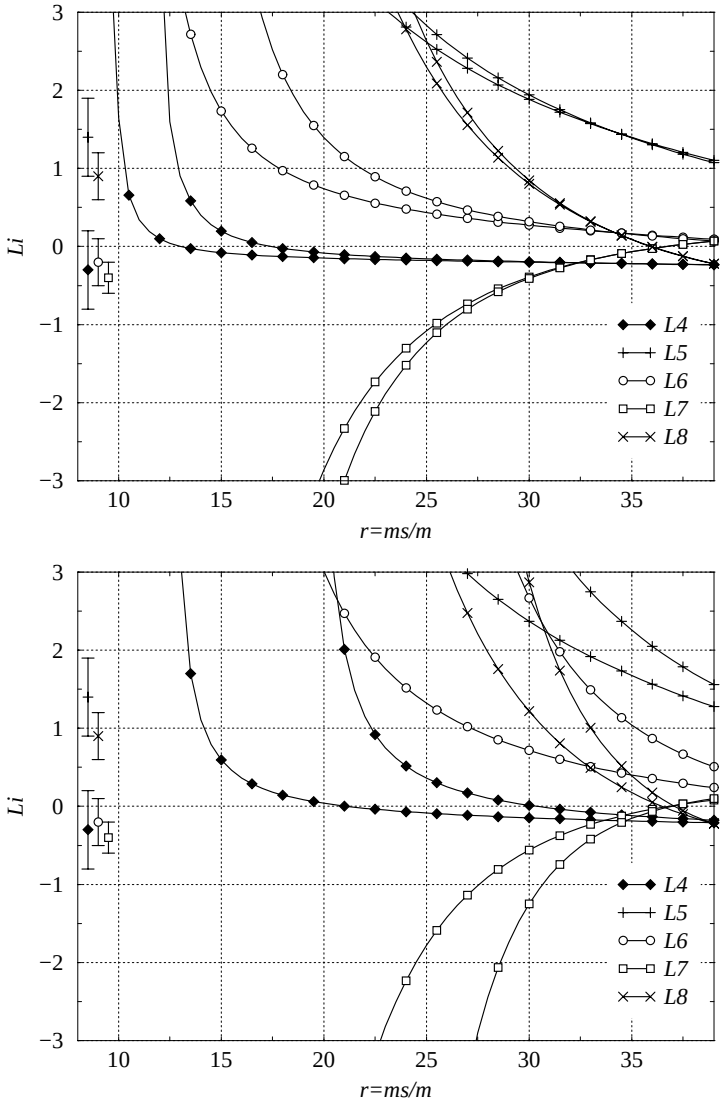

Figure 9: Sum rule: low-energy constants $L_{i=4,\ldots,8}(M_\rho)\cdot 10^3$ as functions of $r = m_s/m$ for $F_0 = 85\,\mathrm{MeV}$, $s_1 = 1.2\,\mathrm{GeV}$ and $s_0 = 1.6\,\mathrm{GeV}$, with the T-matrix models of refs. [31] (up) and [32] (down). The values plotted on the left, along the vertical axis, are the Standard estimates stemming from ref. [3].

The results of the sum rule for $X(3)$ can be converted into bounds for $L_{i=4,\ldots,8}$, plotted on figures 9 and 10 as functions of r, for $\sqrt{s_1} = 1.2\,\mathrm{GeV}$, $\sqrt{s_0} = 1.6\,\mathrm{GeV}$, and $F_0 = 85\,\mathrm{MeV}$. For small r, the LEC's reach very large values: their definition from the low-energy behavior of QCD correlators includes $1/B_0$ factors that make them diverge when $X(3) \to 0$. We notice also the large values of L_5, L_7 and L_8 for $r \sim 25$, because the sum rule pushes $L_6(M_\rho)$ towards slightly *positive* values. The value of L_4 is not predicted by the sum rule: it depends essentially on the value fixed for F_0. For instance, choosing $F_0 = 75\,\mathrm{MeV}$ would yield a slightly positive value for L_4 as r becomes large.

JHEP03(2001)002

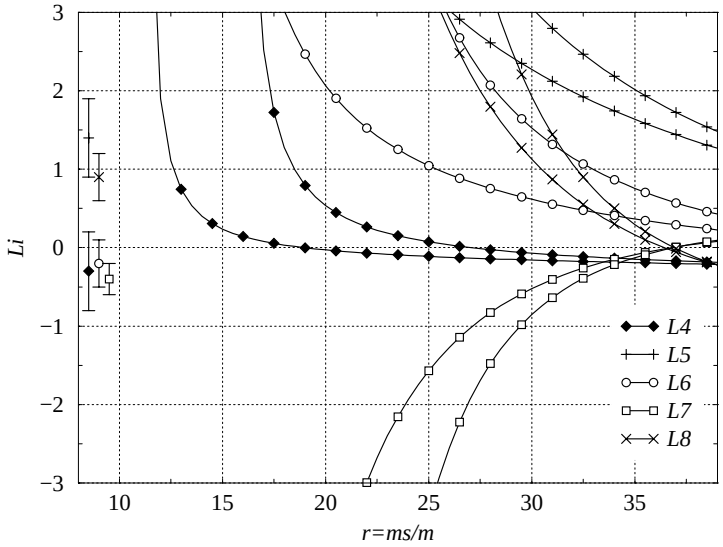

Figure 10: Sum rule: low-energy constants $L_{i=4,\ldots,8}(M_\rho)\cdot 10^3$ as functions of $r = m_s/m$ for $F_0 = 85\,\mathrm{MeV}$, $s_1 = 1.2\,\mathrm{GeV}$ and $s_0 = 1.6\,\mathrm{GeV}$, with the T-matrix models of refs. [33]. The values plotted on the left, along the vertical axis, are the Standard estimates stemming from ref. [3].

We have plotted on the left side of figures 9 and 10 the values of the LEC's of ref. [3], which were derived assuming that $X(3)$ is of order 1 and $L_4(M_\eta) = L_6(M_\eta) = 0$. Let us remind that the values obtained for L_5, L_7, and L_8 are strongly dependent on these assumptions. The values of the LEC's of ref. [3] hardly agree with the ones obtained from the sum rule, because the latter leads to positive values of $L_6(M_\rho)$ and to a small three-flavor condensate.

6.3 Slope of the strange scalar form factor of the pion

Additional information about the decay constants is provided by the scalar form factors through a low-energy theorem. Consider the correlator:

$$D^{ij}_{\mu\nu}(p,q) = \lim_{m\to 0}\int\int e^{i(p\cdot x - q\cdot y)}\langle 0|T\{A^i_\mu(x)\ A^j_\nu(0)\ \bar{s}s(y)|0\rangle^{(c)}\,, \tag{6.5}$$

where $i,j = 1,\ldots,3$, and (c) denotes the connected part of $(A^i_\mu A^j_\nu)(\bar{s}s)$. The Ward identities $p^\mu D^{ij}_{\mu\nu} = r^\nu D^{ij}_{\mu\nu} = 0$ (with $r = q - p$) yield the Lorentz decomposition:

$$\begin{aligned} D^{ij}_{\mu\nu} = m_s\delta_{ij}\Big\{K[r^2 p_\mu p_\nu - (p\cdot r)p_\mu r_\nu + p^2 r_\mu r_\nu - p^2 r^2 g_{\mu\nu}] + \\ + L[r_\mu p_\nu - (p\cdot r)g_{\mu\nu}]\Big\}, \end{aligned} \tag{6.6}$$

where K and L are scalar functions of p^2, q^2 and r^2.

On the one hand, we have:

$$D^{ij}_{\mu\nu}(p,0) = \frac{\partial}{\partial m_s}\left[i\int d^4x e^{ip\cdot x}\langle 0|T\{A^i_\mu(x)\ A^j_\nu(0)\}|0\rangle\right]. \tag{6.7}$$

The correlator $A^i_\mu A^j_\nu$ admits the following decomposition:

$$i\int d^4x e^{ip\cdot x}\langle 0|T\{A^i_\mu(x)\ A^j_\nu(0)\}|0\rangle = \delta^{ij}[p_\mu p_\nu - p^2 g_{\mu\nu}]\Phi(p^2)\,. \tag{6.8}$$

$\Phi(p^2)$ contains a pole at $p^2=0$ stemming from one-pion states:

$$\Phi(p^2) = -\frac{F^2(2)}{p^2} + \cdots\,, \tag{6.9}$$

where the dots denote contributions from the other states. We have therefore:

$$D^{ij}_{\mu\nu}(p,0) = -\delta^{ij}[p_\mu p_\nu - g_{\mu\nu}p^2]\left\{\frac{1}{p^2}\frac{\partial F^2(2)}{\partial m_s} + \cdots\right\}. \tag{6.10}$$

On the other hand, $T^{ij}_{\mu\nu}$ is dominated at low energy by the exchange of two pions between $\bar{s}s$ and each of the axial currents:

$$D^{ij}_{\mu\nu} = 2\delta^{ij}F^2(2)G_1(q^2)\frac{p_\mu r_\nu}{p^2 r^2 (p\cdot r)} + \cdots\,, \tag{6.11}$$

which contributes to K:

$$K(p^2,q^2,r^2) = -2F^2(2)\frac{G_1(q^2)}{p^2 r^2 (p\cdot r)} + \cdots\,, \tag{6.12}$$

whereas $L(p^2,q^2,r^2)$ receives no contribution. We compare eqs. (6.10) and (6.12) for $p,q\to 0$ to obtain:

$$\frac{\partial F^2(2)}{\partial m_s} = 2F^2(2)\lim_{q^2\to 0}\frac{G_1(q^2)}{q^2} \qquad \frac{m_s}{F(2)}\frac{\partial F(2)}{\partial m_s} = m_s G_1'(0)\,. \tag{6.13}$$

This low-energy theorem [17, 18, 26] provides a relation between the logarithmic derivative of $F(2)$ with respect to m_s, and the slope of the strange scalar form factor of the pion for a vanishing momentum.

We can now exploit the solutions of Omnès-Muskhelishvili equations. According to eq. (5.15), we get for the slope of the form factor:

$$m_s G_1'(0) = m_s G_2(0) B_1'(0) = m_s \frac{\partial \bar{M}_K^2}{\partial m_s} B_1'(0) = \lambda_K M_K^2 B_1'(0)\,. \tag{6.14}$$

$B_1'(0)$ is computed by taking the derivative of eq. (5.14) with respect to s at 0:

$$B_1'(0) = \frac{1}{\pi}\sum_{j=1}^{2}\int_{4M_\pi^2}^{\infty} ds' \frac{1}{s'^2} T^*_{1j}(s')\sqrt{\frac{s'-4M_j^2}{s'}}\theta(s'-4M_j^2)B_j(s')\,. \tag{6.15}$$

The numerical resolution of Omnès-Muskhelishvili equations eq. (5.14) yields the values of $\vec{B}(s)$ at the points of integration used for the Gauss-Legendre quadrature [17]. Hence, we can compute directly the integral eq. (6.15) by the same integration method.

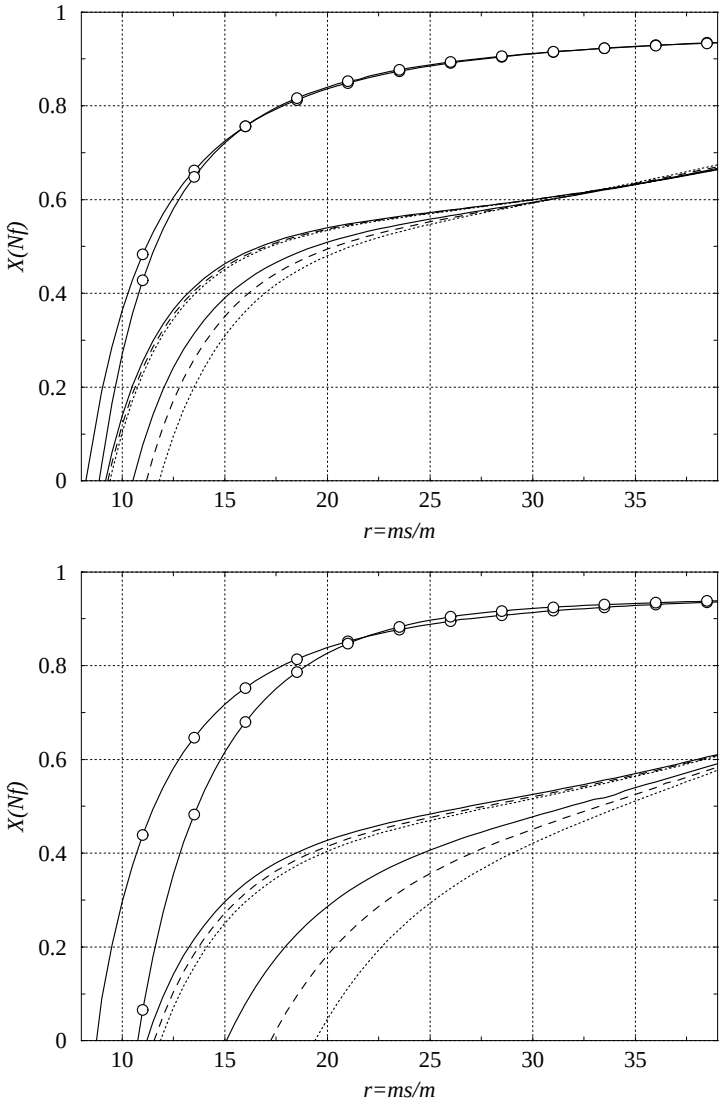

Figure 11: Sum rule and slope of the strange form factor of the pion: range for $X(3)$ as a function of $r = m_s/m$ with the T-matrix models of refs. [31] (up) and [32] (down). The results are plotted for $s_1 = 1.2\,\mathrm{GeV}$ and $s_0 = 1.5\,\mathrm{GeV}$ (solid lines), $1.6\,\mathrm{GeV}$ (dashed lines) and $1.7\,\mathrm{GeV}$ (dotted lines). The lines with white circles show the corresponding range for $X(2)$.

On the other hand, eq. (3.1) leads to:

$$\frac{m_s}{2F^2(2)}\frac{\partial F^2(2)}{\partial m_s} = \frac{1}{\bar{F}_\pi^2}\left[m_s\tilde{\xi} - \frac{rX(3)}{64\pi^2}\frac{F_\pi^2 M_\pi^2}{F_0^2}\left(\log\frac{\bar{M}_K^2}{M_K^2} + \frac{M_K^2}{\bar{M}_K^2}\lambda_K\right)\right]. \qquad (6.16)$$

We see that eq. (6.13) is an additional constraint, different from the sum rule eq. (5.3). From the analysis of the pseudoscalar spectrum, we have concluded that all the quantities could be expressed (at the NLO) as functions of masses, decay constants, and 3 parameters $F_0, r, X(3)$. The sum rule was a first constraint, fixing

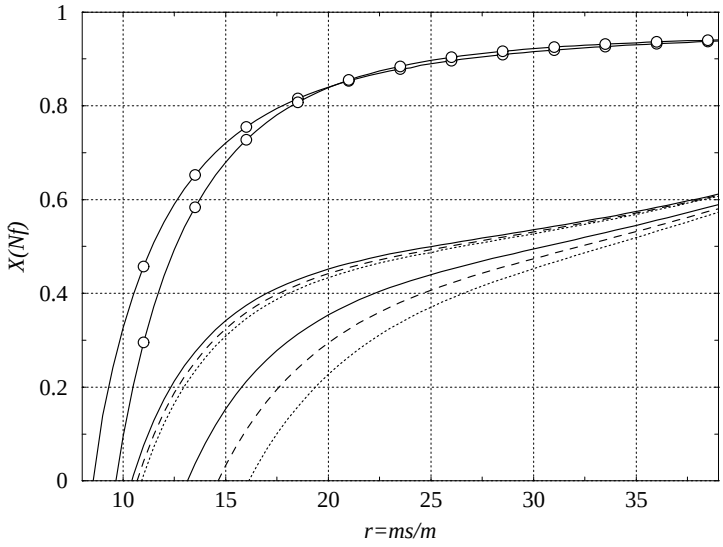

Figure 12: Sum rule and slope of the strange form factor of the pion: range for $X(3)$ as a function of $r = m_s/m$ with the T-matrix models of ref. [33]. The results are plotted for $s_1 = 1.2\,\mathrm{GeV}$ and $s_0 = 1.5\,\mathrm{GeV}$ (solid lines), $1.6\,\mathrm{GeV}$ (dashed lines) and $1.7\,\mathrm{GeV}$ (dotted lines). The lines with white circles show the corresponding range for $X(2)$.

a range for $X(3)$ depending on r and $F_0 \equiv F(3)$. If we exploit the second constraint eq. (6.13), we can obtain ranges for $X(3)$ and $F(3)$ as functions of r, plotted respectively in figures 11–12 and figures 13–14. These results can also be converted into values for the low-energy constants (see figures 15 and 16).

The values of $X(3)$ are close to the ones obtained by the only application of the sum rule eq. (5.3). The results obtained then for $X(3)$ were not very sensitive to the valued chosen for F_0. We see also that the slope of the strange scalar form factor of the pion leads to rather small values for $F(3) \equiv F_0$ (around $70\,\mathrm{MeV}$) for $r \sim 25$. This result is in agreement with the small *positive* values obtained for $L_4(M_\rho)$. This increase of L_4 (with respect to the previous analysis) comes with a decrease of L_5. In ref. [26], the analysis of the same form factor led to $d_F = m_s/F(2) \cdot \partial \log F(2)/\partial m_s = 0.09$. In the framework of Standard χPT, such a value corresponds to $L_4(M_\rho) \simeq 0.4 \cdot 10^{-3}$, i.e. $F(3)$ of order $75\,\mathrm{MeV}$. This question has also been discussed in refs. [17, 18, 27].

However, these two constraints do not demand the same accuracy for the scalar form factors. The sum rule involves the integral of the spectral function $\mathrm{Im}\,\Pi$ up to $1.2\,\mathrm{GeV}$, which is dominated by the $f_0(980)$ peak. The global shape of the spectral function (and more precisely around $1\,\mathrm{GeV}$) is the crucial element. For the low-energy theorem, we are interested in the slope of a form factor at zero, i.e. low-energy details. The resulting constraint may be less stable than the sum rule. It seemed therefore preferable to split the analysis in two parts: the first one dealing only with the sum rule, the second one exploiting both constraints at the same time.

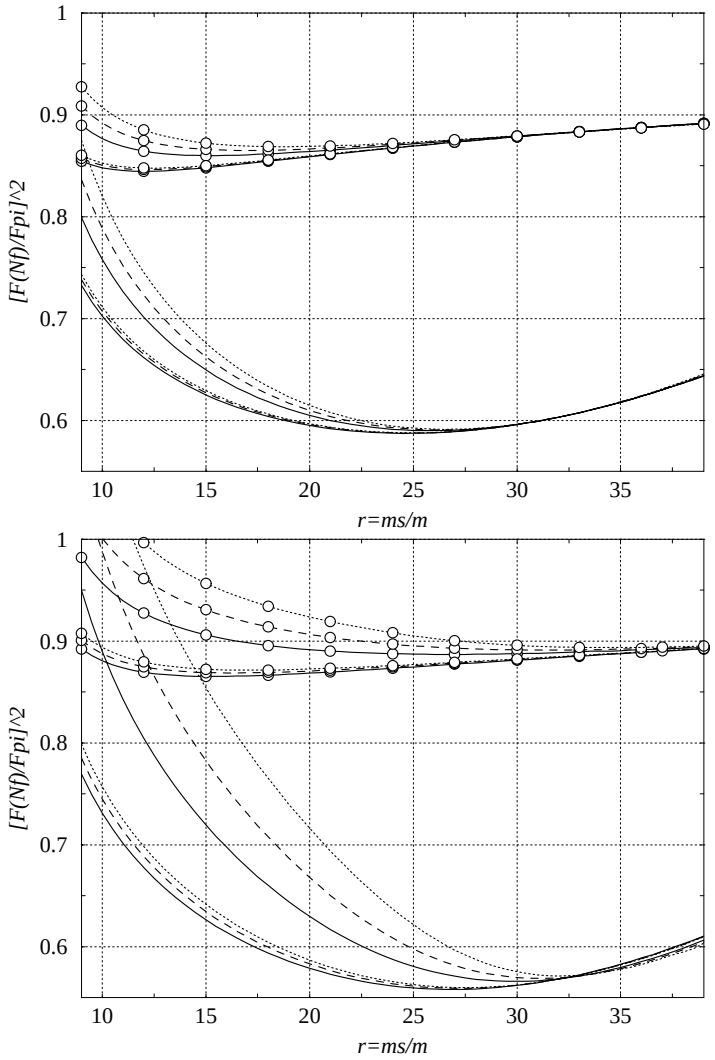

Figure 13: Sum rule and slope of the strange form factor of the pion: ranges for $[F(3)/F_\pi]^2$ (no symbol) and $[F(2)/F_\pi]^2$ (white circles) as functions of $r = m_s/m$ with the T-matrix models of refs. [31] (up) and [32] (down). The results are plotted for $s_1 = 1.2\,\mathrm{GeV}$ and $s_0 = 1.5\,\mathrm{GeV}$ (solid lines), $1.6\,\mathrm{GeV}$ (dashed lines) and $1.7\,\mathrm{GeV}$ (dotted lines).

6.4 Scalar radius of the pion

The scalar radius of the pion $\langle r^2\rangle_s^\pi$ can also be obtained from the scalar form factors of the pion, considered out of the chiral limit (i.e. with the physical masses m_s and $m = (m_u + m_d)/2$):

$$F_1(s) = F_1(0)\left[1 + \frac{1}{6}\langle r^2\rangle_s^\pi s + c_\pi s^2 + \cdots\right], \tag{6.17}$$

If we project $\vec{F}$ on the two solutions $\vec{A}$ and $\vec{B}$, we obtain:

$$\langle r^2\rangle_s^\pi = 6\frac{F_1'(0)}{F_1(0)} = 6\left[A_1'(0) + \frac{M_K^2}{M_\pi^2}\frac{\tilde{\gamma}_K}{\tilde{\gamma}_\pi}B_1'(0)\right], \tag{6.18}$$

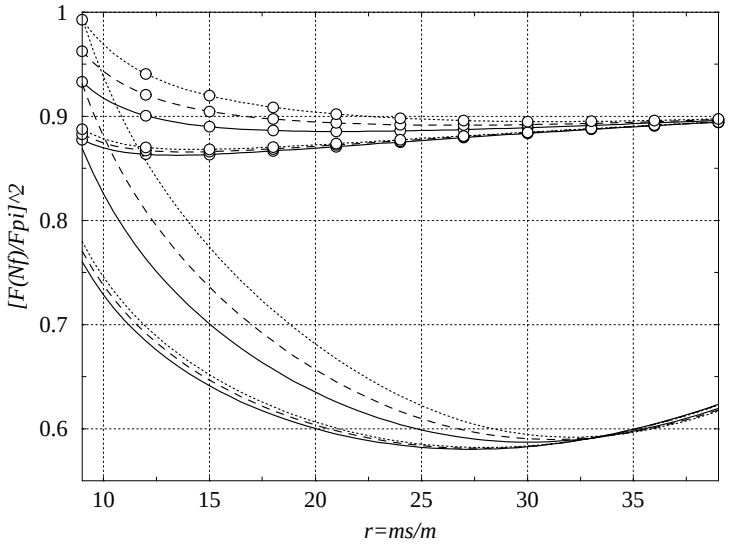

Figure 14: Sum rule and slope of the strange form factor of the pion: ranges for $[F(3)/F_\pi]^2$ (no symbol) and $[F(2)/F_\pi]^2$ (white circles) as functions of $r = m_s/m$ with the T-matrix model of refs. [33]. The results are plotted for $s_1 = 1.2\,\mathrm{GeV}$ and $s_0 = 1.5\,\mathrm{GeV}$ (solid lines), 1.6 GeV (dashed lines) and 1.7 GeV (dotted lines).

where a third kind of logarithmic derivatives is involved (considered out of the chiral limit): $\tilde{\gamma}_P = \partial[\log M_P^2]/\partial[\log m]$. Appendix C.2 collects their expressions in terms of the low-energy constants.

We are interested in a quantity describing the non-strange pion form factor around the threshold. It should be possible to neglect the $K\bar{K}$ channel with no major change in the results. This point of view is supported by a numerical estimate: $B_1'(0)/A_1'(0) \sim 0.1$ and $(M_K^2/M_\pi^2) \times (\tilde{\gamma}_K/\tilde{\gamma}_\pi) \sim 1/2$. If we restricted our analysis to the $\pi\pi$ channel, only the first term (the solution $\vec{A}$) would appear on the right side of eq. (6.18). The scalar radius of the pion would be independent of r, $X(3)$ and F_0 in that case. Actually, the second term on the right side of eq. (6.18), related to the $K\bar{K}$ channel, is responsible for a weak dependence of $\langle r^2\rangle_s^\pi$ on r, $X(3)$, F_0. We can use the previous results, where $X(3)$ and F_0 are functions of r, in order to study the range of variation for the pion scalar radius:

$0.537 - 0.588\,\mathrm{fm}^2$	Oller-Oset-Pelaez	ref. [31],
$0.567 - 0.630\,\mathrm{fm}^2$	Au-Morgan-Pennington	ref. [32],
$0.592 - 0.650\,\mathrm{fm}^2$	Kaminski-Lesniak-Maillet	ref. [33],

to be compared to the estimates: $0.6 \pm 0.2\,\mathrm{fm}^2$ [37], $0.55 \pm 0.15\,\mathrm{fm}^2$ [1], 0.55 to $0.61\,\mathrm{fm}^2$ [30], 0.57 to $0.61\,\mathrm{fm}^2$ [38] and $0.61 \pm 0.04\,\mathrm{fm}^2$ [39]. Notice that the matching of Roy equations with Standard χPT [39] relies strongly on the value of the scalar radius of the pion.

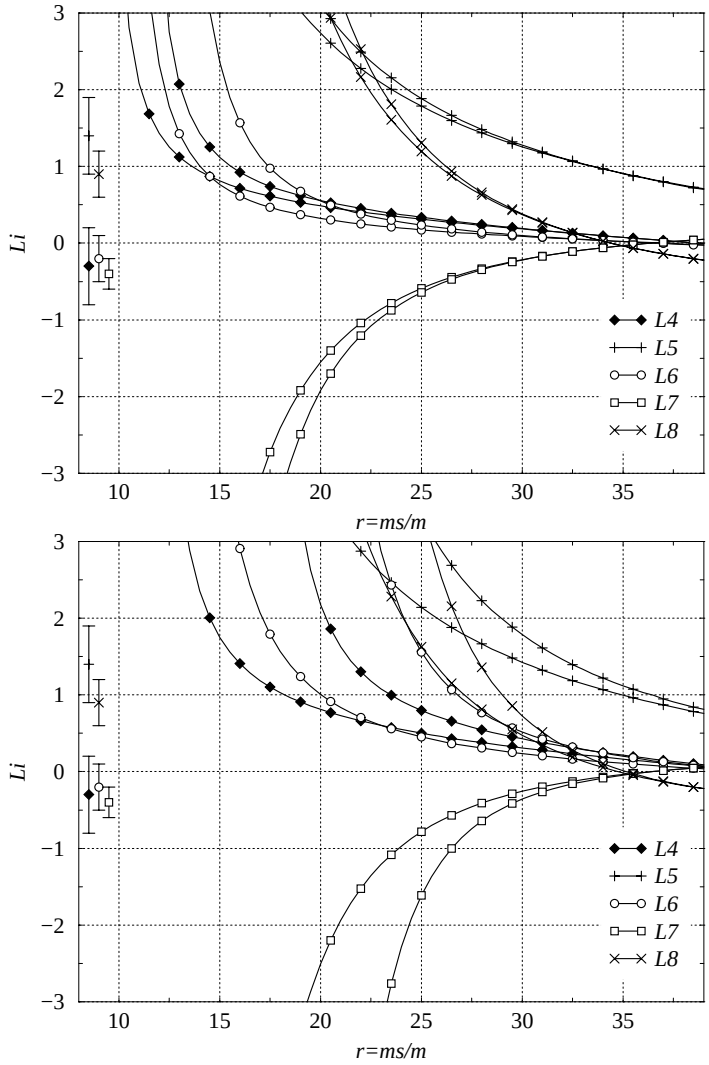

Figure 15: Sum rule and slope of the strange form factor of the pion: low-energy constants $L_{i=4,\ldots,8}(M_\rho)\cdot 10^3$ as functions of $r = m_s/m$ for $F_0 = 85\,\mathrm{MeV}$, $s_1 = 1.2\,\mathrm{GeV}$ and $s_0 = 1.6\,\mathrm{GeV}$, with the T-matrix models of refs. [31] (up) and [32] (down). The values plotted on the left, along the vertical axis, are the Standard estimates stemming from ref. [3].

Information about the scalar radius of the pion could be seen as an additional constraint on our system, since $\langle r^2\rangle_s^\pi$ is related to $2L_4+L_5$. The situation is similar to d_F: this kind of constraint could rather easily be affected by higher-order corrections. We are also obliged to consider it out of the chiral limit $m \to 0$. It seems therefore wiser not to use this constraint, until a new analysis would treat less crudely NNLO remainders.

7. Conclusions

The LEC's of the effective chiral lagrangian should be determined as accurately as possible in order to know and understand the pattern of SBχS. These constants

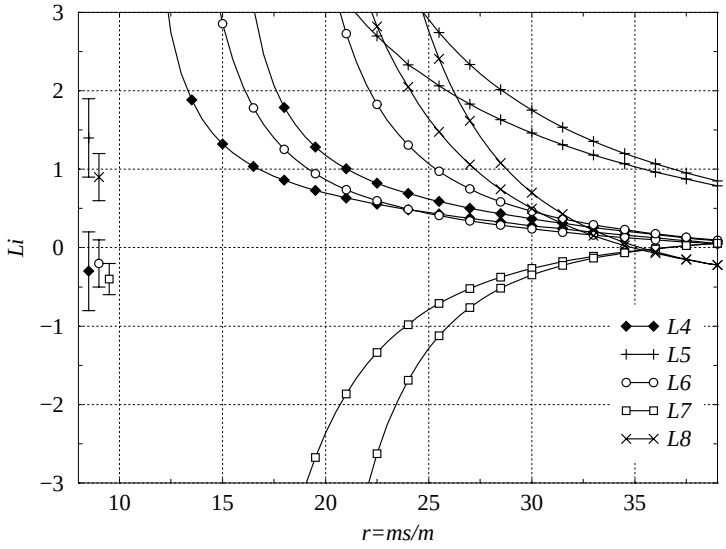

Figure 16: Sum rule and slope of the strange form factor of the pion: low-energy constants $L_{i=4,\ldots,8}(M_\rho) \cdot 10^3$ as functions of $r = m_s/m$ for $F_0 = 85\,\mathrm{MeV}$, $s_1 = 1.2\,\mathrm{GeV}$ and $s_0 = 1.6\,\mathrm{GeV}$, with the T-matrix model of ref. [33]. The values plotted on the left, along the vertical axis, are the Standard estimates stemming from ref. [3].

have generally been estimated from the expansion of Goldstone boson observables in powers of quark masses, supposing (1) a dominance of the quark condensate and (2) an agreement with the large-N_c picture of QCD. But such determinations of the LEC's could be modified if quantum fluctuations turned out to be significant. A symptom of large quantum fluctuations could be seen in the large violation of the Zweig rule in the scalar channel and in large variations of chiral order parameters (e.g. the quark condensate) from $N_f = 2$ to $N_f = 3$.

First we have studied how the relaxation of the Standard assumptions (1) and (2) could affect the determination of the LEC's. To reach this goal, we have studied the expansion in quark masses of the Goldstone boson masses and decay constants. We have truncated these expansions to keep the first two powers in quark masses and we have supposed that higher-order remainders ($O(m^3_{\mathrm{quark}})$ for $F_P^2 M_P^2$ and $O(m^2_{\mathrm{quark}})$ for F_P^2) are small. These expansions can be written using "effective" scale-independent constants that combine chiral logarithms and LEC's. $F_P^2 M_P^2$ involves $\Sigma(3)$, $F^2(3)$ and constants related to L_6, L_7 and L_8, whereas F_P^2 is expressed in terms of $F^2(3)$ and constants corresponding to L_4 and L_5.

We have not considered these expansions in one-loop Standard χPT, since the three-flavor quark condensate $\Sigma(3)$ is not supposed to dominate the expansion of pseudoscalar masses. We have not worked either in tree-level Generalized χPT, since we have included chiral logarithms. These relations between LEC's and experimental quantities (masses and decay constants) can be inverted to express $L_{i=4,\ldots,8}$ (and therefore $X(2)$ and $F(2)$) as functions of $F(3)$, $r = m_s/m$ and $X(3)$. We have

then studied a possible competition between the first two orders of the quark mass expansions, by admitting large values for the ZR violating constants L_4 and L_6 (larger than the expected values on the basis of large-N_c arguments).

The variation of the Gell-Mann–Oakes–Renner ratio X from $N_f = 2$ to $N_f = 3$ is governed by L_6. The equality $X(2) = X(3)$ (saturation of the paramagnetic bound) is realized for $L_6(M_\rho) = -0.21 \cdot 10^{-3}$. A three-flavor GOR ratio $X(3)$ much smaller than 1 could be obtained for two different reasons. On the one hand, the ratio of quark masses r may be smaller than 25 ($r < 20$), which leads to small values of $X(2)$, and then of $X(3)$ (due to the paramagnetic inequality $X(2) \geq X(3)$). On the other hand, $L_6(M_\rho)$ may be larger than the value $-0.26 \cdot 10^{-3}$ saturating the paramagnetic bound for X. A slight shift of $L_6(M_\rho)$ towards positive values leads to a significant decrease of $X(3)$, whereas $X(2)$ remains almost constant and unsuppressed. $X(2)$ could thus be of order 1 and $X(3)$ much smaller than 1, provided that r is large ($r \sim 25$) and the Zweig rule is strongly violated for the correlator defining L_6.

A similar analysis has been performed for the decay constants. L_4 tunes the difference between $F^2(2)$ and $F^2(3)$: the equality is obtained for $L_4(M_\rho) = -0.37 \cdot 10^{-3}$. If $L_4(M_\rho)$ is heading for positive values, $F^2(2)$ and $F^2(3)$ split swiftly. For $r = 25$, the saturation of both paramagnetic inequalities (for F^2 and X) yields $X(2) = X(3) = 0.9$ and $F(2) = F(3) = 87\,\mathrm{MeV}$. This "ultra-Standard" scenario corresponds to the minimal values of L_4 and L_6 (no ZR violation). A slight drift towards positives values could lead to very different chiral structures of the vacuum for $N_f = 2$ and $N_f = 3$, corresponding to a significant role of quantum fluctuations in SBχS.

The pseudoscalar spectrum (masses and decay constants) by itself does not contain enough information to pin down the size of these fluctuations. This effect can however be estimated from experimental data in the scalar channel, through a sum rule. The difference between $X(2)$ and $X(3)$ is related to the correlator Π of two scalar densities $\bar{u}u$ and $\bar{s}s$ at vanishing momentum. $\Pi(0)$ can be expressed in terms of a sum rule made of three distinct integrals. (i) We compute the first one, involving the spectral function $\mathrm{Im}\,\Pi$ up to energies around 1.2 GeV, by solving coupled Omnès-Muskhelishvili equations for the scalar form factors of the pion and the kaon. The solutions depend on the T-matrix model used to describe the interactions between $\pi\pi$- and $\bar{K}K$-channels, and on a normalization of the form factors related to the derivatives of M_π and M_K with respect to m and m_s. (ii) The second integral corresponds to the contribution of the spectral function $\mathrm{Im}\,\Pi$ between 1.2 and 1.6 GeV, where we cannot trust the two-channel approximation anymore. A second sum rule is used to estimate roughly this integral. (iii) The third integral is performed on a large complex circle, with a large enough radius to rely on the Operator Product Expansion (OPE) of Π.

The most significant contribution stems from the first integral: the $f_0(980)$-peak leads to a large value for $\Pi(0)$, and therefore to an important splitting between $X(2)$

and $X(3)$. If we fix $X(3)$, r and $F(3)$, we know $X(2)$ and the LEC's $L_{i=4,\ldots,8}$, using our previous analysis of the pseudoscalar spectrum. The derivatives of M_π and M_K with respect to m and m_s can then be directly computed, since they involve $X(3)$, r, $F(3)$ and LEC's. The sum rule eq. (5.3) can therefore be seen as a constraint, giving $X(3)$ as a function of r and $F(3)$. Several sources of errors could affect this sum rule: the higher-order remainders in the expansions of $F_P^2 M_P^2$ and F_P^2, the rough estimate of the integral in the intermediate energy range, the T-matrix model. The three models considered here support nevertheless a large decrease of $X(3)$ with respect to $X(2)$, corresponding to positive values of $L_6(M_\rho)$. The size of the splitting between the quark condensates depends on the height of the $f_0(980)$ peak in the spectral function. In the particular case of "Standard" inputs $r \sim 25$, $F_0 = 85\,\mathrm{MeV}$, the results of ref. [17] are confirmed: $X(3)$ can hardly reach more than one half of $X(2)$ for the three considered models.[6]

The scalar form factors of the pion and the kaon can be exploited in several different ways. For instance, L_4 (i.e. $F(3)$) is related to the slope of the scalar form factor of the pion at zero. This second constraint may be used to fix $X(3)$ and F_0 as functions of r. If the conclusions for $X(3)$ remain unchanged, positive values of $L_4(M_\rho)$ are obtained, leading to a significant decrease from $F(2)$ to $F(3)$ (20 to 30%). The Zweig rule would be violated strongly for L_4 and L_6. However, this second constraint is sensitive to fine details of a form factor (slope at zero), whereas the sum rule depends on the general shape of the spectral function $\mathrm{Im}\,\Pi$ (and especially on the presence of a high peak corresponding to the $f_0(980)$ resonance). The scalar radius of the pion has also been computed, in agreement with former estimates.

A large decrease of the quark condensate from 2 to 3 flavors could be understood in terms of chiral phase transitions [13]. One of these transitions could be triggered by a vanishing quark condensate. If the corresponding critical value $n_{\mathrm{crit}}(N_c)$ turned out to be close to 2-3, we should expect significant variations of the quark condensate with N_f in the vicinity of the critical point. Moreover, in terms of eigenmodes of the Dirac operator, the quark condensate can be interpreted as a density of eigenvalues, whereas L_6 corresponds to fluctuations of this density. Near the critical point where the first vanishes, the latter is expected to increase significantly. Let us remind that this scenario is only a possible explanation for a large difference between $X(2)$ and $X(3)$. The large value of ZR violating LEC's might be caused by another (and unrelated) mechanism.

Forthcoming experiments [40] on $\pi\pi$ scattering should pin down the value of $X(2)$, which is strongly correlated to r. If $X(2)$ turned out to be close to 1, they could also measure low-energy constants of the $\mathrm{SU}(2) \times \mathrm{SU}(2)$ lagrangian, l_3 and l_4 [1, 41]. However, these experimental values could not be used to fix $\mathrm{SU}(3) \times \mathrm{SU}(3)$

[6] We remind however that this result is barely consistent with the Standard hypothesis of a three-flavor condensate dominating the description of SBχS.

LEC's without assumptions on the size of the ZR violating LEC's L_4 and L_6 [13]. It would be possible to constrain more tightly L_6 through a more sophisticated analysis of the sum rule including bounds on $X(2)$ (or equivalently r). However, this remains a very indirect determination of the three-flavor condensate. Direct experimental tests are necessary to investigate closely the chiral structure of QCD vacuum for three massless quarks, and to understand the role of quantum fluctuations in the pattern of SBχS.

Acknowledgments

I thank J. Stern for suggesting this problem and for constant help and support, B. Moussallam for many useful explanations and for providing his program solving numerically Omnès-Muskhelishvili equations, P. Talavera for a careful reading of the manuscript, and M. Knecht, U.-G. Meißner, E. Oset and H. Sazdjian for various discussions and comments. Work partly supported by the EU, TMR-CT98-0169, EURODAΦNE network.

A. Spectrum of pseudoscalar mesons

A.1 Decay constants

The decay constants are [1, 36]:

$$
\begin{aligned}
F_\pi^2 &= F_0^2 + 2m\xi + 2(2m+m_s)\tilde{\xi} + \frac{1}{16\pi^2}\frac{F_\pi^2 M_\pi^2}{F_0^2} X(3)\left[2\log\frac{M_K^2}{M_\pi^2} + \log\frac{M_\eta^2}{M_K^2}\right] + \varepsilon_\pi\,,\\
F_K^2 &= F_0^2 + (m+m_s)\xi + 2(2m+m_s)\tilde{\xi} + \frac{1}{2}\frac{F_\pi^2 M_\pi^2}{F_0^2} X(3) L + \varepsilon_K\,,\\
F_\eta^2 &= F_0^2 + \frac{2}{3}(m+2m_s)\xi + 2(2m+m_s) + \tilde{\xi} + \frac{1}{48\pi^2}\frac{F_\pi^2 M_\pi^2}{F_0^2}(2r+1) X(3)\log\frac{M_\eta^2}{M_K^2} + \varepsilon_\eta\,,
\end{aligned}
\tag{A.1}
$$

with the scale-independent low-energy constants:

$$
\begin{aligned}
\xi &= F_0^2\xi(\mu) - \frac{B_0}{32\pi^2}\left(\log\frac{M_K^2}{\mu^2} + 2\log\frac{M_\eta^2}{\mu^2}\right)\\
&= 8B_0\left[L_5(\mu) - \frac{1}{256\pi^2}\left(\log\frac{M_K^2}{\mu^2} + 2\log\frac{M_\eta^2}{\mu^2}\right)\right],\\
\tilde{\xi} &= F_0^2\tilde{\xi}(\mu) - \frac{B_0}{32\pi^2}\log\frac{M_K^2}{\mu^2}\\
&= 8B_0\left[L_4(\mu) - \frac{1}{256\pi^2}\log\frac{M_K^2}{\mu^2}\right],
\end{aligned}
\tag{A.2}
$$

and:

$$
L = \frac{1}{32\pi^2}\left[3\log\frac{M_K^2}{M_\pi^2} + \log\frac{M_\eta^2}{M_K^2}\right]. \tag{A.3}
$$

The higher-order contributions are denoted by $\delta_2 F_P^2$. The effective constants are related to F_0 through the relations:

$$
\begin{aligned}
m_s\xi &= \frac{r}{r-1}\left\{F_K^2 - F_\pi^2 + \frac{1}{64\pi^2}\frac{F_\pi^2 M_\pi^2}{F_0^2}X(3)\left[5\log\frac{M_K^2}{M_\pi^2} + 3\log\frac{M_\eta^2}{M_K^2}\right]\right\} + \\
&\quad + \frac{r}{r-1}\left[\varepsilon_\pi - \varepsilon_K\right], \\
m_s\tilde{\xi} &= \frac{r}{2(r+2)}\left\{\frac{r+1}{r-1}F_\pi^2 - \frac{2}{r-1}F_K^2 - F_0^2 - \right. \\
&\qquad \left. - \frac{1}{32\pi^2}\frac{F_\pi^2 M_\pi^2}{F_0^2}X(3)\left[\frac{4r+1}{r-1}\log\frac{M_K^2}{M_\pi^2} + \frac{2r+1}{r-1}\log\frac{M_\eta^2}{M_K^2}\right]\right\} + \\
&\quad + \frac{r}{2(r+2)}\left[\frac{2}{r-1}\varepsilon_K - \frac{r+1}{r-1}\varepsilon_\pi\right].
\end{aligned}
\tag{A.4}
$$

The decay constants fulfill the relation:

$$
\begin{aligned}
F_\eta^2 &= \frac{4}{3}F_K^2 - \frac{1}{3}F_\pi^2 + \frac{1}{24\pi^2}\frac{M_\pi^2 F_\pi^2}{F_0^2}rX(3)\log\frac{M_\eta^2}{M_K^2} + \\
&\quad + \frac{1}{48\pi^2}\frac{M_\pi^2 F_\pi^2}{F_0^2}X(3)\left(\log\frac{M_\eta^2}{M_K^2} - \log\frac{M_K^2}{M_\pi^2}\right) + \varepsilon_\eta - \frac{4}{3}\varepsilon_K + \frac{1}{3}\varepsilon_\pi\,.
\end{aligned}
\tag{A.5}
$$

A.2 Masses

The pseudoscalar masses are [1, 36]:

$$
F_\pi^2 M_\pi^2 = 2m\Sigma + (2mm_s + 4m^2)Z^S + 4m^2 A + \frac{F_\pi^4 M_\pi^4}{F_0^4}[X(3)]^2 L + F_\pi^2\delta_\pi\,, \tag{A.6}
$$

$$
\begin{aligned}
F_K^2 M_K^2 &= (m_s+m)\Sigma + (m_s+m)(m_s+2m)Z^S + (m_s+m)^2 A + \\
&\quad + \frac{1}{4}\frac{F_\pi^4 M_\pi^4}{F_0^4}(r+1)[X(3)]^2 L + F_K^2\delta_K\,,
\end{aligned}
\tag{A.7}
$$

$$
\begin{aligned}
F_\eta^2 M_\eta^2 &= \frac{2}{3}(2m_s+m)\Sigma + \frac{2}{3}(2m_s+m)(m_s+2m)Z^S + \\
&\quad + \frac{4}{3}(2m_s^2+m^2)A + \frac{8}{3}(m_s-m)^2 Z^P + \\
&\quad + \frac{1}{3}\frac{F_\pi^4 M_\pi^4}{F_0^4}[X(3)]^2 L + F_\eta^2\delta_\eta\,.
\end{aligned}
\tag{A.8}
$$

with the scale-independent low-energy constants:

$$
\begin{aligned}
Z^S &= 2F_0^2 Z_0^S(\mu) - \frac{B_0^2}{32\pi^2}\left\{2\log\frac{M_K^2}{\mu^2} + \frac{4}{9}\log\frac{M_\eta^2}{\mu^2}\right\} \\
&= 32B_0^2\left[L_6(\mu) - \frac{1}{512\pi^2}\left\{\log\frac{M_K^2}{\mu^2} + \frac{2}{9}\log\frac{M_\eta^2}{\mu^2}\right\}\right], \\
A &= F_0^2 A_0(\mu) - \frac{B_0^2}{32\pi^2}\left\{\log\frac{M_K^2}{\mu^2} + \frac{2}{3}\log\frac{M_\eta^2}{\mu^2}\right\}
\end{aligned}
$$

$$= 16B_0^2\left[L_8(\mu) - \frac{1}{512\pi^2}\left\{\log\frac{M_K^2}{\mu^2} + \frac{2}{3}\log\frac{M_\eta^2}{\mu^2}\right\}\right],$$
$$Z^P = F_0^2 Z_0^P = 16B_0^2 L_7\,. \tag{A.9}$$

The higher-order remainders are denoted by δM_P^2. The low-energy constants can be estimated using the relations:

$$\begin{aligned}
m_s^2 Z^S &= F_\pi^2 M_\pi^2 \frac{r^2}{2(r+2)}\left\{1 - \tilde{\epsilon}(r) - X(3) - \frac{F_\pi^2 M_\pi^2}{F_0^4}\frac{r[X(3)]^2}{r-1}L\right\} + \\
&\quad + \frac{r^2}{2(r+2)}\left[\frac{4}{r^2-1}F_K^2\delta_K - \frac{r+1}{r-1}F_\pi^2\delta_\pi\right], \\
m_s^2 A &= F_\pi^2 M_\pi^2 \frac{r^2}{4}\left\{\tilde{\epsilon}(r) + \frac{F_\pi^2 M_\pi^2}{F_0^4}\frac{[X(3)]^2}{r-1}L\right\} + \\
&\quad + \frac{r^2}{2(r-1)}F_\pi^2\delta_\pi - \frac{r^2}{r^2-1}F_K^2\delta_K\,, \\
m_s^2 Z^P &= \frac{r^2}{8}\left\{\frac{1}{(r-1)^2}\left[3F_\eta^2 M_\eta^2 + F_\pi^2 M_\pi^2 - 4F_K^2 M_K^2\right] - F_\pi^2 M_\pi^2\tilde{\epsilon}(r)\right\} - \\
&\quad - \frac{r^2}{8(r-1)^2}\left[3F_\eta^2\delta_\eta + \frac{8r}{r+1}F_K^2\delta_K + (2r-1)F_\pi^2\delta_\pi\right],
\end{aligned} \tag{A.10}$$

with:

$$\tilde{\epsilon}(r) = 2\frac{\tilde{r}_2 - r}{r^2-1} \qquad \tilde{r}_2 = 2\frac{F_K^2 M_K^2}{F_\pi^2 M_\pi^2} - 1\,. \tag{A.11}$$

A.3 Pseudoscalar masses for $m \to 0$

From the previous relations, one can derive low-energy constants from experimental data (pseudoscalar masses, F_π and F_K) and 3 parameters: r, $X(3)$ and F_0.

$$\begin{aligned}
F_\pi, F_K &\to \quad F_\eta, m_s\xi, m_s\tilde{\xi} \quad \to \bar{F}_\pi, \bar{F}_K, \bar{F}_\eta \\
M_\pi, M_K, M_\eta &\to m_s^2 Z^S, m_s^2 A, m_s^2 Z^P \to \bar{M}_K, \bar{M}_\eta\,.
\end{aligned} \tag{A.12}$$

In the chiral limit $m \to 0$, we will have to know the effective constants:

$$\lim_{m\to 0} X_i = X_i + \sum_P C_P \cdot \log\frac{\bar{M}_P^2}{M_P^2}\,. \tag{A.13}$$

To compute $\bar{M}_P$ in this expression, we take the chiral limit of the mass expansions eqs. (A.6)–(A.8). But these expansions involve the effective constants at $m = 0$, which leads to corrections containing logarithms of $\bar{M}_Q/M_Q$:

$$\bar{M}_P = \sum_i a_i X_i + \sum_Q D_Q \cdot \log\frac{\bar{M}_Q^2}{M_Q^2}\,. \tag{A.14}$$

The equations eq. (A.14) could be solved iteratively. Actually, $\bar{M}_Q/M_Q$ remains very close to 1. The calculation is simplified (and still accurate) if we compute in

a slightly different way $\bar{M}_Q$ in the logarithmic piece of eq. (A.14). We start from eq. (A.14), and we neglect the second (logarithmic) term:

$$\bar{M}_Q = \sum_i a_i X_i \,. \tag{A.15}$$

$\bar{M}_Q$ is then directly computed from observables and $F_0, r, X(3)$. We put then these values of $\bar{M}_Q$ in the logarithmic term of eq. (A.14). We end up with values of $\bar{M}_P$ very close to the ones computed iteratively. These values will be used to compute the low-energy constants in the chiral limit $X_i|_{m=0}$ using eq. (A.13).

B. Operator product expansion for Π

Six integrals contribute to the Wilson coefficient of $m_s\langle\bar{u}u\rangle$ at the leading order in the strong coupling constant. The corresponding Feynman diagrams are drawn on figure 5. On each line, the left and right diagrams correspond to each other by crossing the gluonic lines. A simple change of variables in the integrals shows that the diagrams on the same line contribute identically to the Wilson coefficient.

We want to consider the large-p^2 behavior of integrals like:

$$J(\{\nu_i\},\{m_i\},p) = \int \frac{d^4q\; d^4k}{[q^2-m_1^2]^{\nu_1}[k^2-m_2^2]^{\nu_2}} \times \\ \times \frac{1}{[(k+q)^2-m_3^2]^{\nu_3}[(p-q)^2-m_4^2]^{\nu_4}[(k+p)^2-m_5^2]^{\nu_5}} \,. \tag{B.1}$$

These integrals are formally identical to the integrals arising in two-loop computations of self-energies, see figure 17.

The behavior of such integrals at large external momentum is known. The basic idea is to follow the flow of this large external momentum through the Feynman diagram, in order to Taylor expand correctly the propagators [24]. This procedure

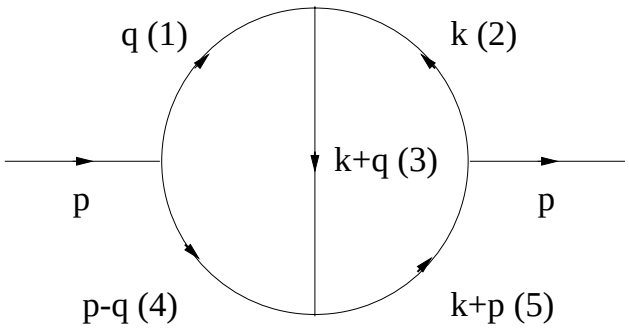

Figure 17: Self-energy diagram, leading to the same kind of integrals as in the OPE of Π at the lowest order.

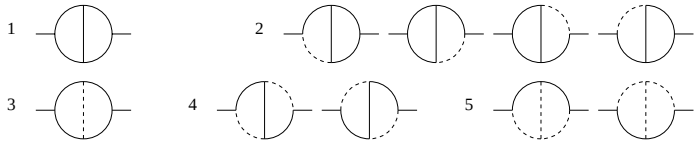

Figure 18: Subgraphs involved in the asymptotic expansion of the two-loop Feynman integrals. The solid lines constitute the subgraphs, the dashed lines correspond to the excluded propagators [24].

relies on the asymptotic expansion theorem [25] and can be formally expressed as:

$$J_\Gamma \underset{p^2\to\infty}{\sim} \sum_\gamma J_{\Gamma/\gamma} \circ \mathcal{T}_{\{m_i\},\{q_i\}} J_\gamma \,. \tag{B.2}$$

Γ denotes the whole graph, γ are subgraphs into which the large external momentum may flow and Γ/γ is the complementary graph of γ. For each subgraph γ (see figure 18), we write the corresponding Feynman integral J_γ. We perform then a Taylor expansion $\mathcal{T}_{\{m_i\},\{q_i\}}$ with respect to the masses and the small momenta (external to γ and not containing p). We combine the resulting "expanded" integral with the remaining graph Γ/γ and integrate over internal momenta. The asymptotic behavior of the whole integral J_Γ is obtained by considering all the possible flows γ for the large external momentum.

We look for the leading order in $1/p^2$ of the Wilson coefficient. All the subraphs do not contribute with the same power of $1/p^2$. In particular, the diagrams of type 5 do not appear in the Wilson coefficient of $m_s\langle\bar{u}u\rangle$ at the leading order in $1/p^2$. Gathering all the contributions, we obtain:

$$\Pi(p^2) \underset{P^2\to\infty}{\sim} \frac{\alpha_s^2 m_s^2}{M_\pi^2 M_K^2} \frac{2}{\pi^2 p^2} \{[5-6\zeta(3)] + [5-6\zeta(3)] - [1+6\zeta(3)]\}\,, \tag{B.3}$$

where the bracketed terms correspond respectively to the contributions of the first, second and third lines in figure 5. The $\zeta(3)$ terms are related to subdiagrams of type 1 (see figure 18), corresponding to two-loop massless integrals $J(\{\nu_i\},\{0\},p)$.

C. Logarithmic derivatives

C.1 Logarithmic derivatives for $m \to 0$

To compute the logarithmic derivatives γ_P and λ_P:

$$\gamma_P = \frac{m}{M_P^2}\left(\frac{\partial M_P^2}{\partial m}\right)_{m=0}, \qquad \lambda_P = \frac{m_s}{M_P^2}\left(\frac{\partial M_P^2}{\partial m_s}\right)_{m=0}, \tag{C.1}$$

we use the relations:

$$\begin{aligned}
\gamma_P &= \frac{m}{\bar{F}_P^2 M_P^2}\left(\frac{\partial[F_P^2 M_P^2]}{\partial m}\right)_{m=0} - \frac{\bar{M}_P^2}{M_P^2}\cdot\frac{m}{\bar{F}_P^2}\left(\frac{\partial F_P^2}{\partial m}\right)_{m=0}, \\
\lambda_P &= \frac{m_s}{\bar{F}_P^2 M_P^2}\frac{\partial[\bar{F}_P^2\bar{M}_P^2]}{\partial m_s} - \frac{\bar{M}_P^2}{M_P^2}\cdot\frac{m_s}{\bar{F}_P^2}\frac{\partial \bar{F}_P^2}{\partial m_s},
\end{aligned} \tag{C.2}$$

where $\bar{X} = \lim_{m\to 0} X$.

The logarithmic derivatives with respect to m are:

$$\gamma_\pi = \frac{1}{\bar{F}_\pi^2 M_\pi^2}\Bigg\{F_\pi^2 M_\pi^2 X(3) + \frac{2}{r}m_s^2 Z^S - \\ - \frac{1}{32\pi^2}\frac{F_\pi^4 M_\pi^4}{F_0^4} r[X(3)]^2\left(\log\frac{\bar{M}_K^2}{M_K^2} + \frac{2}{9}\log\frac{\bar{M}_\eta^2}{M_\eta^2}\right)\Bigg\} + \\ + \frac{m}{\bar{F}_\pi^2 M_\pi^2}\left(\frac{\partial[F_\pi^2\delta_\pi]}{\partial m}\right)_{m=0},$$

$$\gamma_K\left[1 - \frac{3}{64\pi^2}\frac{F_\pi^2 M_\pi^2}{F_0^2\bar{F}_K^2} rX(3) + \frac{3}{128\pi^2}\frac{M_\pi^4 F_\pi^4}{F_0^4}\frac{1}{\bar{F}_K^2\bar{M}_K^2}[rX(3)]^2\right] + \\ + \gamma_\eta\left[-\frac{1}{32\pi^2}\frac{F_\pi^2 M_\pi^2}{F_0^2\bar{F}_K^2}\frac{M_\eta^2\bar{M}_K^2}{\bar{M}_\eta^2 M_K^2} rX(3) + \frac{5}{576\pi^2}\frac{M_\pi^4 F_\pi^4}{F_0^4}\frac{1}{\bar{F}_K^2 M_K^2}\frac{M_\eta^2}{\bar{M}_\eta^2}[rX(3)]^2\right] = \\ = \frac{1}{\bar{F}_K^2 M_K^2}\Bigg\{\frac{F_\pi^2 M_\pi^2}{2}X(3) + \frac{1}{r}\left[3m_s^2 Z^S + 2m_s^2 A - \bar{M}_K^2\left(m_s\xi + 4m_s\tilde{\xi}\right)\right] + \\ - \frac{1}{16\pi^2}\frac{F_\pi^4 M_\pi^4}{F_0^4} r[X(3)]^2\left[\log\frac{\bar{M}_K^2}{M_K^2} + \frac{1}{3}\log\frac{\bar{M}_\eta^2}{M_\eta^2}\right] + \\ + \frac{1}{64\pi^2}\frac{F_\pi^2 M_\pi^2}{F_0^2}\bar{M}_K^2 X(3)\left[5\log\frac{\bar{M}_K^2}{M_K^2} + 2\log\frac{\bar{M}_\eta^2}{M_\eta^2}\right]\Bigg\} + \\ + \frac{m}{\bar{F}_K^2 M_K^2}\left(\frac{\partial[F_K^2\delta_K]}{\partial m}\right)_{m=0} - \frac{\bar{M}_K^2}{M_K^2}\cdot\frac{m}{\bar{F}_K^2}\left(\frac{\partial\varepsilon_K}{\partial m}\right)_{m=0},$$

$$\gamma_K\left[-\frac{3}{32\pi^2}\frac{F_\pi^2 M_\pi^2}{F_0^2\bar{F}_\eta^2}\frac{M_K^2\bar{M}_\eta^2}{\bar{M}_K^2 M_\eta^2} rX(3) + \frac{1}{24\pi^2}\frac{F_\pi^4 M_\pi^4}{F_0^4}\frac{1}{\bar{F}_\eta^2 M_\eta^2}\frac{M_K^2}{\bar{M}_K^2}[rX(3)]^2\right] + \\ + \gamma_\eta\left[1 + \frac{1}{54\pi^2}\frac{F_\pi^4 M_\pi^4}{F_0^4}\frac{1}{\bar{F}_\eta^2\bar{M}_\eta^2}[rX(3)]^2\right] = \\ = \frac{1}{\bar{F}_\eta^2 M_\eta^2}\Bigg\{\frac{F_\pi^2 M_\pi^2}{3}X(3) + \\ + \frac{1}{r}\left[\frac{10}{3}m_s^2 Z^S + \frac{16}{3}m_s^2 Z^P - \bar{M}_\eta^2\left(\frac{2}{3}m_s\xi + 4m_s\tilde{\xi}\right)\right] - \\ - \frac{1}{32\pi^2}\frac{F_\pi^4 M_\pi^4}{F_0^4} r[X(3)]^2\left[\frac{5}{3}\log\frac{M_K^2}{\bar{M}_K^2} + \frac{10}{27}\log\frac{M_\eta^2}{\bar{M}_\eta^2}\right] - \\ - \frac{1}{32\pi^2}\frac{F_\pi^2 M_\pi^2}{F_0^2}\bar{M}_\eta^2 X(3)\left[7\log\frac{\bar{M}_K^2}{M_K^2} + 2\log\frac{\bar{M}_\eta^2}{M_\eta^2} + 2\log\frac{\bar{M}_K^2}{\bar{M}_\eta^2}\right]\Bigg\} + \\ + \frac{m}{\bar{F}_\eta^2 M_\eta^2}\left(\frac{\partial[F_\eta^2\delta_\eta]}{\partial m}\right)_{m=0} - \frac{\bar{M}_\eta^2}{M_\eta^2}\cdot\frac{m}{\bar{F}_\eta^2}\left(\frac{\partial\varepsilon_\eta}{\partial m}\right)_{m=0}. \qquad \text{(C.3)}$$

The logarithmic derivatives with respect to m_s are:

$$\lambda_\pi = 0\,,$$

$$\begin{aligned}
&\lambda_K\left[1-\frac{3}{64\pi^2}\frac{F_\pi^2M_\pi^2}{F_0^2\bar F_K^2}rX(3)+\frac{3}{128\pi^2}\frac{F_\pi^4M_\pi^4}{F_0^4}\frac{1}{\bar F_K^2\bar M_K^2}[rX(3)]^2\right]+\\
&\quad+\lambda_\eta\left[-\frac{1}{32\pi^2}\frac{F_\pi^2M_\pi^2}{F_0^2\bar F_K^2}\frac{\bar M_K^2M_\eta^2}{M_K^2\bar M_\eta^2}rX(3)+\frac{5}{576\pi^2}\frac{F_\pi^4M_\pi^4}{F_0^4}\frac{1}{\bar F_K^2M_K^2}\frac{M_\eta^2}{\bar M_\eta^2}[rX(3)]^2\right]=\\
&\qquad=\frac{1}{\bar F_K^2M_K^2}\left\{\frac{F_\pi^2M_\pi^2}{2}rX(3)+2m_s^2Z^S+2m_s^2A-\bar M_K^2(m_s\xi+2m_s\tilde\xi)-\right.\\
&\qquad\qquad-\frac{1}{128\pi^2}\frac{F_\pi^4M_\pi^4}{F_0^4}[rX(3)]^2\left[5\log\frac{\bar M_K^2}{M_K^2}+\frac{20}{9}\log\frac{\bar M_\eta^2}{M_\eta^2}\right]+\\
&\qquad\qquad\left.+\frac{1}{64\pi^2}\frac{F_\pi^2M_\pi^2}{F_0^2}\bar M_K^2rX(3)\left[3\log\frac{\bar M_K^2}{M_K^2}+2\log\frac{\bar M_\eta^2}{M_\eta^2}\right]\right\}+\\
&\qquad+\frac{m_s}{\bar F_K^2M_K^2}\left(\frac{\partial[F_K^2\delta_K]}{\partial m_s}\right)_{m=0}-\frac{\bar M_K^2}{M_K^2}\cdot\frac{m_s}{\bar F_K^2}\left(\frac{\partial\varepsilon_K}{\partial m_s}\right)_{m=0},
\end{aligned}$$

$$\begin{aligned}
&\lambda_K\left[-\frac{3}{32\pi^2}\frac{F_\pi^2M_\pi^2}{F_0^2\bar F_\eta^2}\frac{M_K^2}{\bar M_K^2}\frac{\bar M_\eta^2}{M_\eta^2}rX(3)+\frac{1}{24\pi^2}\frac{F_\pi^4M_\pi^4}{F_0^4}\frac{1}{\bar F_\eta^2M_\eta^2}\frac{M_K^2}{\bar M_K^2}[rX(3)]^2\right]+\\
&\quad+\lambda_\eta\left[1+\frac{1}{54\pi^2}\frac{F_\pi^4M_\pi^4}{F_0^4}\frac{1}{\bar F_\eta^2\bar M_\eta^2}[rX(3)]^2\right]=\\
&\qquad=\frac{1}{\bar F_\eta^2M_\eta^2}\left\{\frac{4F_\pi^2M_\pi^2}{3}rX(3)+\right.\\
&\qquad\qquad+\frac{8}{3}\left[m_s^2Z^S+2m_s^2A+2m_s^2Z^P\right]-\bar M_\eta^2\left(\frac{4}{3}m_s\xi+2m_s\tilde\xi\right)-\\
&\qquad\qquad-\frac{1}{12\pi^2}\frac{F_\pi^4M_\pi^4}{F_0^4}[rX(3)]^2\left[\log\frac{\bar M_K^2}{M_K^2}+\frac{4}{9}\log\frac{\bar M_\eta^2}{M_\eta^2}\right]+\\
&\qquad\qquad\left.+\frac{1}{96\pi^2}\frac{F_\pi^2M_\pi^2}{F_0^2}\bar M_\eta^2rX(3)\left[5\log\frac{\bar M_K^2}{M_K^2}+4\log\frac{\bar M_\eta^2}{M_\eta^2}+4\log\frac{\bar M_K^2}{\bar M_\eta^2}\right]\right\}+\\
&\qquad+\frac{m_s}{\bar F_\eta^2M_\eta^2}\left(\frac{\partial[F_\eta^2\delta_\eta]}{\partial m_s}\right)_{m=0}-\frac{\bar M_\eta^2}{M_\eta^2}\cdot\frac{m_s}{\bar F_\eta^2}\left(\frac{\partial\varepsilon_\eta}{\partial m_s}\right)_{m=0}.
\end{aligned}\tag{C.4}$$

C.2 Logarithmic derivatives for $m \neq 0$

The same method can be used to compute the logarithmic derivatives involved in the scalar radius of the pion:

$$\tilde\gamma_P=\frac{m}{M_P^2}\frac{\partial M_P^2}{\partial m}.\tag{C.5}$$

We obtain:

$$\begin{aligned}
\tilde{\gamma}_\pi = & \frac{1}{F_\pi^2 M_\pi^2}\left\{F_\pi^2 M_\pi^2 X(3) + \frac{2}{r^2}\left[(r+4)m_s^2 Z^S + 4m_s^2 A\right] - \frac{2M_\pi^2}{r}[m_s\xi + 2m_s\tilde{\xi}]\right\} + \\
& + \frac{F_\pi^2 M_\pi^2}{F_0^4}\frac{[X(3)]^2}{32\pi^2}\left[6\log\frac{M_K^2}{M_\pi^2} + 2\log\frac{M_\eta^2}{M_K^2} - 3\tilde{\gamma}_\pi - (r+1)\tilde{\gamma}_K - \frac{1}{9}(2r+1)\tilde{\gamma}_\eta\right] - \\
& - \frac{M_\pi^2}{F_0^2}\frac{X(3)}{32\pi^2}\left[4\log\frac{M_K^2}{M_\pi^2} + 2\log\frac{M_\eta^2}{M_K^2} - 4\tilde{\gamma}_\pi - (r+1)\tilde{\gamma}_K\right] + \\
& + \frac{m}{F_\pi^2 M_\pi^2}\frac{\partial[F_\pi^2\delta_\pi]}{\partial m} - \frac{m}{F_\pi^2}\frac{\partial\varepsilon_\pi}{\partial m},
\end{aligned}$$

$$\begin{aligned}
\tilde{\gamma}_K = & \frac{1}{F_K^2 M_K^2}\left\{\frac{F_\pi^2 M_\pi^2}{2}X(3) + \frac{3r+4}{r^2}m_s^2 Z^S + \frac{2(r+1)}{r^2}m_s^2 A - \frac{M_K^2}{r}[m_s\xi + 4m_s\tilde{\xi}]\right\} + \\
& + \frac{F_\pi^4 M_\pi^4}{F_0^4 F_K^2 M_K^2}\frac{[X(3)]^2}{128\pi^2}\left[3(r+2)\log\frac{M_K^2}{M_\pi^2} + (r+2)\log\frac{M_\eta^2}{M_K^2} - \right. \\
& \qquad \left. - 3\tilde{\gamma}_\pi - 3(r+1)^2\tilde{\gamma}_K - \frac{5}{9}(2r+1)(r+1)\tilde{\gamma}_\eta\right] - \\
& - \frac{F_\pi^2 M_\pi^2}{F_K^2 F_0^2}\frac{X(3)}{64\pi^2}\left[3\log\frac{M_K^2}{M_\pi^2} + \log\frac{M_\eta^2}{M_K^2} - 3\tilde{\gamma}_\pi - 3(r+1)\tilde{\gamma}_K - (2r+1)\tilde{\gamma}_\eta\right] + \\
& + \frac{m}{F_K^2 M_K^2}\frac{\partial[F_K^2\delta_K]}{\partial m} - \frac{m}{F_K^2}\frac{\partial\varepsilon_K}{\partial m},
\end{aligned}$$

$$\begin{aligned}
\tilde{\gamma}_\eta = & \frac{1}{F_\eta^2 M_\eta^2}\left\{\frac{F_\pi^2 M_\pi^2}{3}X(3) + \frac{2(4+5r)}{3r^2}m_s^2 Z^S + \frac{8}{3r^2}m_s^2 A - \right. \\
& \qquad \left. - \frac{16(r-1)}{3r^2}m_s^2 Z^P - \frac{M_\eta^2}{r}\left[\frac{2}{3}m_s\xi + 4m_s\tilde{\xi}\right]\right\} + \\
& + \frac{F_\pi^4 M_\pi^4}{F_0^4 F_\eta^2 M_\eta^2}\frac{[X(3)]^2}{128\pi^2}\left[8\log\frac{M_K^2}{M_\pi^2} + \frac{8}{3}\log\frac{M_\eta^2}{M_K^2} - 4\tilde{\gamma}_\pi - \right. \\
& \qquad \left. - \frac{4}{3}(4r+1)(r+1)\tilde{\gamma}_K - \frac{4}{27}(16r^2+10r+1)\tilde{\gamma}_\eta\right] - \\
& - \frac{F_\pi^2 M_\pi^2}{F_\eta^2 F_0^2}\frac{X(3)}{64\pi^2}\left[\frac{4}{3}\log\frac{M_\eta^2}{M_K^2} - 6(r+1)\tilde{\gamma}_K\right] + \\
& + \frac{m}{F_\eta^2 M_\eta^2}\frac{\partial[F_\eta^2\delta_\eta]}{\partial m} - \frac{m}{F_\eta^2}\frac{\partial\varepsilon_\eta}{\partial m}.
\end{aligned} \tag{C.6}$$

This linear system of three equations and three variables is easily solved to compute $\tilde{\gamma}_\pi$ and $\tilde{\gamma}_K$ as functions of F_0, r and $X(3)$.

References

[1] J. Gasser and H. Leutwyler, *Chiral perturbation theory to one loop*, *Ann. Phys. (NY)* **158** (1984) 142; *Chiral perturbation theory: expansions in the mass of the strange quark*, *Nucl. Phys.* **B 250** (1985) 465.

[2] *The second DAΦNE physics handbook*, L. Maiani, G. Pancheri and N. Paver eds., INFN, Frascati, Italy 1995.

[3] J. Bijnens, G. Ecker and J. Gasser, *Chiral perturbation theory*, hep-ph/9411232.

[4] G. Ecker, J. Gasser, A. Pich and E. de Rafael, *The role of resonances in chiral perturbation theory*, *Nucl. Phys.* **B 321** (1989) 311.

[5] M. Knecht and E. de Rafael, *Patterns of spontaneous chiral symmetry breaking in the large-N_c limit of QCD-like theories*, *Phys. Lett.* **B 424** (1998) 335 [hep-ph/9712457]; S. Peris, M. Perrottet and E. de Rafael, *Matching long and short distances in large-N_c QCD*, *J. High Energy Phys.* **05** (1998) 011 [hep-ph/9805442]; M.F. L. Golterman and S. Peris, *The 7/11 rule: an estimate of m_ρ/f_π*, *Phys. Rev.* **D 61** (2000) 034018 [hep-ph/9908252].

[6] G. Amoros, J. Bijnens and P. Talavera, *$K_{\ell 4}$ form-factors and π-π scattering*, *Nucl. Phys.* **B 585** (2000) 293 [hep-ph/0003258].

[7] S. Coleman and E. Witten, *Chiral symmetry breakdown in large-N chromodynamics*, *Phys. Rev. Lett.* **45** (1980) 100; G. 't Hooft, *A planar diagram theory for strong interactions*, *Nucl. Phys.* **B 72** (1974) 461; *A two-dimensional model for mesons*, *Nucl. Phys.* **B 75** (1974) 461; G.C. Rossi and G. Veneziano, *A possible description of baryon dynamics in dual and gauge theories*, *Nucl. Phys.* **B 123** (1977) 507; E. Witten, *Baryons in the 1/N expansion*, *Nucl. Phys.* **B 160** (1979) 57.

[8] S. Spanier and N. Tornqvist, *Note on scalar mesons: in review of particle physics (RPP 1998)*, *Eur. Phys. J.* **C 3** (1998) 390; For a recent discussion, M.R. Pennington, *Riddle of the scalars: where is the sigma?*, hep-ph/9905241, and references therein.

[9] Y. Iwasaki, K. Kanaya, S. Kaya, S. Sakai and T. Yoshie, *Quantum chromodynamics with many flavors*, *Prog. Theor. Phys. Suppl.* **131** (1998) 415 [hep-lat/9804005]; D. Chen and R.D. Mawhinney, *Dependence of QCD hadron masses on the number of dynamical quarks*, *Nucl. Phys.* **53** *(Proc. Suppl.)* (1997) 216 [hep-lat/9705029]; R.D. Mawhinney, *Evidence for pronounced quark loop effects in QCD*, *Nucl. Phys.* **60A** *(Proc. Suppl.)* (1998) 306 [hep-lat/9705031]; C. Zhong Sui, *QCD with zero, two and four flavors of light quarks: results from QCDSP*, *Nucl. Phys.* **73** *(Proc. Suppl.)* (1999) 228 [hep-lat/9811011]; P.H. Damgaard, U.M. Heller, A. Krasnitz and P. Olesen, *On lattice QCD with many flavors*, *Phys. Lett.* **B 400** (1997) 169 [hep-lat/9701008].

JHEP03(2001)002

[10] E. Gardi and G. Grunberg, *The conformal window in QCD and supersymmetric QCD*, *J. High Energy Phys.* **03** (1999) 024 [hep-th/9810192].

[11] T. Appelquist, A. Ratnaweera, J. Terning and L.C. R. Wijewardhana, *The phase structure of an* SU(N) *gauge theory with* N_f *flavors*, *Phys. Rev.* **D 58** (1998) 105017 [hep-ph/9806472].

[12] T. Appelquist and S.B. Selipsky, *Instantons and the chiral phase transition*, *Phys. Lett.* **B 400** (1997) 364 [hep-ph/9702404];
M. Velkovsky and E. Shuryak, *QCD with large number of quarks: effects of the instanton anti-instanton pairs*, *Phys. Lett.* **B 437** (1998) 398 [hep-ph/9703345].

[13] S. Descotes, L. Girlanda and J. Stern, *Paramagnetic effect of light quark loops on chiral symmetry breaking*, *J. High Energy Phys.* **01** (2000) 041 [hep-ph/9910537].

[14] T. Banks and A. Casher, *Chiral symmetry breaking in confining theories*, *Nucl. Phys.* **B 169** (1980) 103.

[15] H. Leutwyler and A. Smilga, *Spectrum of dirac operator and role of winding number in QCD*, *Phys. Rev.* **D 46** (1992) 5607;
S. Descotes and J. Stern, *Finite-volume analysis of* N_f*-induced chiral phase transitions*, *Phys. Rev.* **D 62** (2000) 054011 [hep-ph/9912234].

[16] J. Stern, *Two alternatives of spontaneous chiral symmetry breaking in QCD*, hep-ph/9801282.

[17] B. Moussallam, N_f *dependence of the quark condensate from a chiral sum rule*, *Eur. Phys. J.* **C 14** (2000) 111 [hep-ph/9909292].

[18] B. Moussallam, *Flavor stability of the chiral vacuum and scalar meson dynamics*, *J. High Energy Phys.* **08** (2000) 005 [hep-ph/0005245].

[19] H. Georgi, *Generalized dimensional analysis*, *Phys. Lett.* **B 298** (1993) 187 [hep-ph/9207278].

[20] S. Descotes and J. Stern, *Vacuum fluctuations of* $\bar{q}q$ *and values of low-energy constants*, *Phys. Lett.* **B 488** (2000) 274 [hep-ph/0007082].

[21] M. Gell-Mann, R.J. Oakes and B. Renner, *Behavior of current divergences under* SU(3) $\times$ SU(3), *Phys. Rev.* **175** (1968) 2195.

[22] M. Knecht and J. Stern, *Generalized chiral perturbation theory*, hep-ph/9411253;
M. Knecht, B. Moussallam, J. Stern and N.H. Fuchs, *The low-energy* $\pi\pi$ *amplitude to one and two loops*, *Nucl. Phys.* **B 457** (1995) 513 [hep-ph/9507319].

[23] M. Gell-Mann, *Symmetries of baryons and mesons*, *Phys. Rev.* **125** (1962) 1067
S. Okubo, *Note on unitary symmetry in strong interactions*, *Prog. Theor. Phys.* **27** (1962) 949.

JHEP03(2001)002

[24] A.I. Davydychev, V.A. Smirnov and J.B. Tausk, *Large momentum expansion of two loop selfenergy diagrams with arbitrary masses*, *Nucl. Phys.* **B 410** (1993) 325 [hep-ph/9307371].

[25] V.A. Smirnov, *Asymptotic expansions in limits of large momenta and masses*, *Comm. Math. Phys.* **134** (1990) 109.

[26] J.F. Donoghue, J. Gasser and H. Leutwyler, *The decay of a light Higgs boson*, *Nucl. Phys.* **B 343** (1990) 341.

[27] U.-G. Meissner and J.A. Oller, *$J/\psi \to \phi\pi\pi(K\bar{K})$ decays, chiral dynamics and ozi violation*, *Nucl. Phys.* **A 679** (2001) 671 [hep-ph/0005253].

[28] R. Omnes, *On the solution of certain singular integral equations of quantum field theory*, *Nuovo Cim.* **8** (1958) 316.

[29] N.I. Muskhelishvili, *Singular integral equations*, Noordhoff, Groningen 1953

[30] J. Gasser and U.G. Meissner, *Chiral expansion of pion form-factors beyond one loop*, *Nucl. Phys.* **B 357** (1991) 90.

[31] J.A. Oller, E. Oset and J.R. Pelaez, *Meson meson and meson baryon interactions in a chiral non-perturbative approach*, *Phys. Rev.* **D 59** (1999) 074001 [hep-ph/9804209].

[32] K.L. Au, D. Morgan and M.R. Pennington, *Meson dynamics beyond the quark model: a study of final state interactions*, *Phys. Rev.* **D 35** (1987) 1633.

[33] R. Kaminski, L. Lesniak and J.P. Maillet, *Relativistic effects in the scalar meson dynamics*, *Phys. Rev.* **D 50** (1994) 3145 [hep-ph/9403264];
R. Kaminski, L. Lesniak and B. Loiseau, *Three channel model of meson meson scattering and scalar meson spectroscopy*, *Phys. Lett.* **B 413** (1997) 130 [hep-ph/9707377].

[34] E. Braaten, S. Narison and A. Pich, *QCD analysis of the tau hadronic width*, *Nucl. Phys.* **B B373** (1992) 581.

[35] V.A. Novikov, M.A. Shifman, A.I. Vainshtein and V.I. Zakharov, *Are all hadrons alike? technical appendices*, *Nucl. Phys.* **B 191** (1981) 301.

[36] N.H. Fuchs, M. Knecht and J. Stern, *Contributions of order $\mathcal{O}(m^2_{\rm quark})$ to $K_{\ell 3}$ form factors and unitarity of the CKM matrix*, *Phys. Rev.* **D 62** (2000) 033003 [hep-ph/0001188].

[37] J. Gasser and H. Leutwyler, *Low-energy theorems as precision tests of QCD*, *Phys. Lett.* **B 125** (1983) 325.

[38] J. Bijnens, G. Colangelo and P. Talavera, *The vector and scalar form factors of the pion to two loops*, *J. High Energy Phys.* **05** (1998) 014 [hep-ph/9805389].

JHEP03(2001)002

[39] B. Ananthanarayan, G. Colangelo, J. Gasser and H. Leutwyler, *Roy equation analysis of $\pi\pi$ scattering*, hep-ph/0005297;
G. Colangelo, J. Gasser and H. Leutwyler, *The $\pi\pi$ s-wave scattering lengths*, *Phys. Lett.* **B 488** (2000) 261 [hep-ph/0007112].

[40] M. Baillargeon and P.J. Franzini, *Accuracies of K_{e4} parameters at DAΦNE*, hep-ph/9407277;
U.-G. Meissner et al., *Working group on $\pi\pi$ and πN interactions*, in Proc. of *Chiral dynamics: theory and experiment*, A.M. Bernstein, D. Drechsel and T. Walcher eds., Mainz, Germany, September 1-5 1997, Springer 1998 [hep-ph/9711361].

[41] J. Bijnens, G. Colangelo, G. Ecker, J. Gasser and M.E. Sainio, *Elastic $\pi\pi$ scattering to two loops*, *Phys. Lett.* **B 374** (1996) 210 [hep-ph/9511397]; *Pion pion scattering at low energy*, *Nucl. Phys.* **B 508** (1997) 263 [hep-ph/9707291];
L. Girlanda, M. Knecht, B. Moussallam and J. Stern, *Comment on the prediction of two-loop standard chiral perturbation theory for low-energy pi pi scattering*, *Phys. Lett.* **B 409** (1997) 461 [hep-ph/9703448];
M. Knecht, B. Moussallam, J. Stern and N.H. Fuchs, *Determination of two-loop $\pi\pi$ scattering amplitude parameters*, *Nucl. Phys.* **B 471** (1996) 445 [hep-ph/9512404].

JHEP03(2001)002